

1   **An antisense RNA capable of modulating the  
2   expression of the tumor suppressor microRNA-34a**  
3

4   **Jason T. Serviss<sup>1\*</sup>, Felix Clemens Richter<sup>1,2</sup>, Jimmy Van Den Eynden<sup>3</sup>,**  
5   **Nathanael Johansson Andrews<sup>1</sup>, Miranda Houtman<sup>1,4</sup>, Laura**  
6   **Schwarzmueller<sup>1</sup>, Per Johnsson, Erik Larsson<sup>3</sup>, Dan Grandér<sup>1</sup>, Katja**  
7   **Pokrovskaja Tamm<sup>1</sup>**

8  
9   <sup>1</sup> Department of Oncology and Pathology, Karolinska Institutet, Stockholm,  
10   Sweden

11   <sup>2</sup> Kennedy Institute of Rheumatology, University of Oxford, Roosevelt Drive,  
12   Oxford OX3 7FY, UK

13   <sup>3</sup>Department of Medical Biochemistry and Cell Biology, Institute of  
14   Biomedicine, The Sahlgrenska Academy, University of Gothenburg, SE-405  
15   30 Gothenburg, Sweden

16   <sup>4</sup> Rheumatology Unit, Department of Medicine, Karolinska University Hospital  
17   Solna, Karolinska Institutet, Stockholm, Sweden

18  
19   **\* Correspondence:**

20   Jason T. Serviss, Department of Oncology and Pathology, Karolinska  
21   Institutet, Stockholm, Sweden, SE-17177. [jason.serviss@ki.se](mailto:jason.serviss@ki.se)

22  
23   **Abstract**

25   The microRNA-34a is a well-studied tumor suppressor microRNA (miRNA)  
26   that is a direct down-stream target of TP53 and has roles in multiple pathways  
27   associated with oncogenesis, such as proliferation, cellular growth, and  
28   differentiation. Due to its wide variety of targets that suppress oncogenesis, it  
29   is not surprising that miR34a expression has been shown to be dys-regulated  
30   in a wide variety of both solid tumors and hematological malignancies.  
31   Despite this, the mechanisms by which miR34a is regulated in these cancers  
32   is not well studied. Here we find that the *miR34a* antisense RNA, a long non-  
33   coding RNA transcribed antisense to *miR34a*, is critical  
34   for *miR34a* expression and mediation of its cellular functions in multiple types  
35   of human cancer. In addition, we characterize miR34a asRNA's ability to  
36   facilitate miR34a expression under multiple types of cellular stress in both

37 *TP53* deficient and wild-type settings.

38 **Introduction**

39 In recent years advances in functional genomics has revolutionized our  
40 understanding of the human genome. Evidence now points to the fact that  
41 approximately 75% of the genome is transcribed but only ~1.2% of this is  
42 responsible for encoding proteins (International Human Genome Sequencing  
43 2004, Djebali et al. 2012). Of these recently identified elements, long non-  
44 coding (lnc) RNAs are defined as transcripts exceeding 200bp in length with a  
45 lack of a functional open reading frame. Some lncRNAs are dually classified  
46 as antisense (as) RNAs that are expressed from the same locus as a sense  
47 transcript in the opposite orientation. Current estimates using high-throughput  
48 transcriptome sequencing, indicate that up to 20-40% of the approximately  
49 20,000 protein-coding genes exhibit antisense transcription (Chen et al. 2004,  
50 Katayama et al. 2005, Ozsolak et al. 2010). The hypothesis that asRNAs play  
51 an important role in oncogenesis was first proposed when studies increasingly  
52 found examples of aberrant expression of these transcripts and other lncRNA  
53 subgroups in tumor samples (Balbin et al. 2015). Although studies  
54 characterizing the functional importance of asRNAs in cancer are limited to  
55 date, characterization a number of individual transcripts has led to the  
56 discovery of multiple examples of asRNA-mediated regulation of several well  
57 known tumorigenic factors (Yap et al. 2010, Johnsson et al. 2013). The  
58 mechanisms by which asRNAs accomplish this are diverse, and include  
59 recruitment of chromatin modifying factors (Rinn et al. 2007), acting as  
60 microRNA (miRNA) sponges (Memczak et al. 2013), and causing  
61 transcriptional interference (Conley et al. 2012).

62  
63 Responses to cellular stress, e.g. DNA damage, sustained oncogene  
64 expression, and nutrient deprivation, are all tightly monitored and orchestrated  
65 cellular pathways that are commonly dys-regulated in cancer. Cellular  
66 signaling in response to these types of cellular stress often converge on the  
67 transcription factor TP53 that regulates transcription of coding and non-coding  
68 downstream targets. One non-coding target of TP53 is the tumor suppressor  
69 microRNA known as *miR34a* (Raver-Shapira et al. 2007).  
70 Upon TP53 activation *miR34a* expression is increased allowing it to down-  
71 regulate its targets involved in cellular pathways such as, growth factor  
72 signaling, apoptosis, differentiation, and cellular senescence (Lal et al. 2011,  
73 Slabakova et al. 2017). *miR34a* is a crucial factor in mediating activated TP53  
74 response and it is often deleted or down-regulated in human cancers and has  
75 also been shown to be a valuable prognostic marker (Cole et al. 2008,  
76 Gallardo et al. 2009, Zenz et al. 2009, Cheng et al. 2010, Liu et al. 2011).  
77 Reduced *miR34a* transcription is mediated via epigenetic regulation in many  
78 solid tumors, such as colorectal-, pancreatic-, and ovarian cancer (Vogt et al.  
79 2011), as well as multiple types of hematological malignancies (Chim et al.  
80 2010). In addition, miR34a has been shown to be transcriptionally regulated  
81 via TP53 homologs, TP63 and TP73, other transcription factors, e.g. STAT3  
82 and MYC, and, in addition, post-transcriptionally through miRNA sponging by  
83 the NEAT1 lncRNA (Chang et al. 2008, Su et al. 2010, Agostini et al. 2011,  
84 Rokavec et al. 2015, Ding et al. 2017). Despite these findings, the  
85 mechanisms underlying miR34a regulation in the context of oncogenesis have  
86 not yet been fully elucidated.

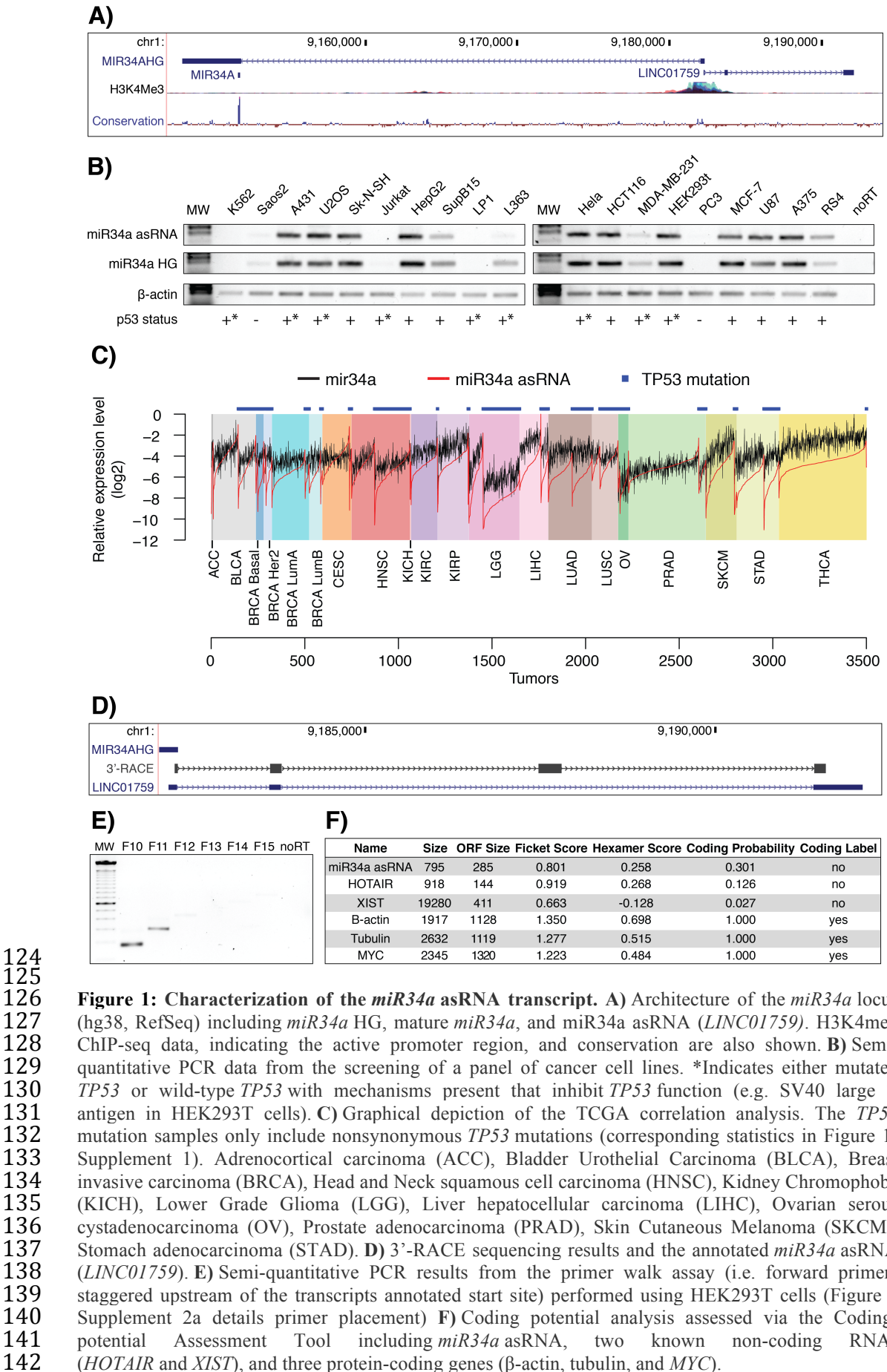
87  
88 Studies across multiple cancer types have reported a decrease in oncogenic  
89 phenotypes when miR34a expression is induced in a p53-null background,  
90 although endogenous mechanisms for achieving this have not yet been  
91 discovered (Liu et al. 2011, Ahn et al. 2012, Yang et al. 2012, Stahlhut et al.  
92 2015, Wang et al. 2015). In addition, previous reports have identified a  
93 lncRNA originating in the antisense orientation from the miR34a locus which  
94 is regulated by TP53 and is induced upon multiple forms of cellular stress  
95 (Rashi-Elkeles et al. 2014, Hunten et al. 2015, Leveille et al. 2015, Ashouri et  
96 al. 2016, Kim et al. 2017). Despite this, none of these studies have continued  
97 to functionally characterize this transcript. In this study we functionally  
98 characterize the *miR34a* asRNA transcript, and find that modulating the levels  
99 of the *miR34a* asRNA is sufficient to increase levels of *miR34a* and results in  
100 a decrease of multiple tumorigenic phenotypes. Furthermore, we find that  
101 *miR34a* asRNA-mediated up-regulation of *miR34a* is sufficient to induce  
102 endogenous cellular mechanisms counteracting several types of stress stimuli  
103 in a *TP53* deficient background. Finally, similar to the functional roles of  
104 antisense transcription at protein-coding genes, we identify a rare example of  
105 an antisense RNA capable of regulating a cancer-associated miRNA.

106

107 **Results**

108  
109 ***miR34a* asRNA is a broadly expressed, non-coding transcript whose**  
110 **levels correlate with *miR34a* expression**  
111  
112 *miR34a* asRNA is transcribed in a “head-to-head” orientation with  
113 approximately 100 base pair overlap with the *miR34a* host gene (HG) (**Fig.**  
114 **1a**). Due to the fact that sense/antisense pairs can be both concordantly and

115 discordantly expressed, we sought to evaluate this relationship in the case of  
116 *miR34a* HG and its asRNA. Using a diverse panel of cancer cell lines, we  
117 detected co-expression of both the *miR34a* HG and *miR34a* asRNA (**Fig. 1b**).  
118 We included *TP53*+/+, *TP53* mutated, and *TP53*-/- cell lines in the panel due  
119 to previous reports that *miR34a* is a known downstream target of TP53.  
120 These results indicate that *miR34a* HG and *miR34a* asRNA are co-expressed  
121 and that their expression levels correlate with *TP53* status, with *TP53*-/- cell  
122 lines tending to have decreased or abolished expression of both transcripts.  
123



143 We next sought to interrogate primary cancer samples to examine if a  
144 correlation between *miR34a* asRNA and *miR34a* expression levels could be  
145 identified. For this task we utilized RNA sequencing data from The Cancer  
146 Genome Atlas (TCGA) after stratifying patients by cancer type, *TP53* status  
147 and, where appropriate, cancer subtypes. The results indicate  
148 that *miR34a* asRNA and *miR34a* expression are strongly correlated in the  
149 vast majority of cancer types examined, both in the presence and absence of  
150 wild-type *TP53* (**Fig. 1c, Figure 1-Figure Supplement 1a**). The results also  
151 further confirm that the expression levels of both *miR34a* and its asRNA tend  
152 to be reduced in patients with nonsynonymous *TP53* mutations (**Figure 1-**  
153 **Figure Supplement 1b**).

154

155 Next, we aimed to gain a thorough understanding of *miR34a* asRNA's  
156 molecular characteristics and cellular localization. To experimentally  
157 determine the 3' termination site for the *miR34a* asRNA transcript we  
158 performed 3' rapid amplification of cDNA ends (RACE) using the U2OS  
159 osteosarcoma cell line that exhibited high endogenous levels  
160 of *miR34a* asRNA in the cell panel screening. Sequencing the cloned cDNA  
161 indicated that the transcripts 3' transcription termination site is 525 base pairs  
162 upstream of the *LINC01759* transcript's annotated termination site (**Fig. 1d**).  
163 Next, we characterized the *miR34a* asRNA 5' transcription start site by  
164 carrying out a primer walk assay, i.e. a common reverse primer was placed in  
165 exon 2 and forward primers were gradually staggered upstream of the  
166 transcripts annotated start site (**Figure 1-Figure Supplement 2a**). Our results  
167 indicated that the 5' start site for *miR34a* asRNA is in fact approximately 90bp

168 (F11 primer) to 220bp (F12 primer) upstream of the annotated start site (**Fig.**  
169 **1e**). Polyadenylation status was evaluated via cDNA synthesis with either  
170 random nanomers or oligoDT primers followed by semi-quantitative PCR with  
171 results indicating that the *miR34a* asRNA is polyadenylated although the  
172 unspliced form seems to only be in the polyA negative state (**Figure 1-Figure**  
173 **Supplement 2b**). We furthermore investigated the propensity  
174 of *miR34a* asRNA to be alternatively spliced in U2OS cells, using PCR  
175 cloning and sequencing and found that the transcript is post-transcriptionally  
176 spliced to form multiple different isoforms (**Figure 1-Figure Supplement 2c**).  
177 Finally, to evaluate the cellular localization of *miR34a* asRNA we utilized RNA  
178 sequencing data from five cancer cell lines included in the ENCODE  
179 (Consortium 2012) project that had been fractionated into cytosolic and  
180 nuclear fractions. The analysis revealed that the *miR34a* asRNA transcript  
181 localizes to both the nucleus and cytoplasm but primarily resides in the  
182 nucleus (**Figure 1-Figure Supplement 2d**).

183

184 Finally, we utilized multiple approaches to evaluate the coding potential of  
185 the *miR34a* asRNA transcript. The Coding-Potential Assessment Tool is a  
186 bioinformatics-based tool that uses a logistic regression model to evaluate  
187 coding-potential by examining ORF length, ORF coverage, Fickett score and  
188 hexamer score (Wang et al. 2013). Results indicated that *miR34a* asRNA has  
189 a similar lack of coding capacity to the known non-coding  
190 transcripts *HOTAIR* and *XIST* and differs greatly when examining these  
191 parameters to the known coding transcripts  $\beta$ -actin, tubulin, and *MYC* (**Fig.**  
192 **1F**). We further confirmed these results using the Coding-Potential Calculator

193 that utilizes a support based machine-based classifier and accesses an  
194 alternate set of discriminatory features (**Figure 1-Figure Supplement 2e**)  
195 (Kong et al. 2007). \*\*\* We hope to be able to scan for peptides matching to  
196 miR34a asRNA in CPTAC and Geiger et al., 2012 before submission and will  
197 mention results here.\*\*\*

198

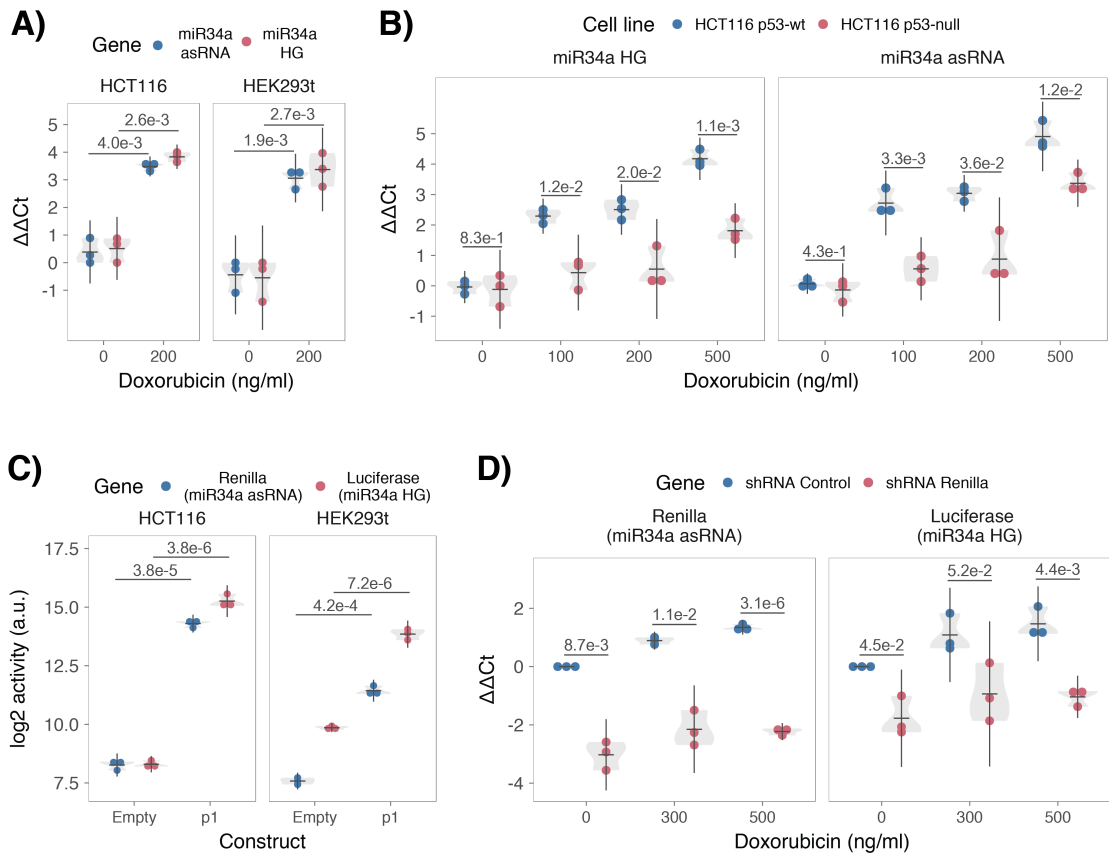
### 199 **TP53-mediated regulation of *miR34a* asRNA expression**

200 *miR34a* is a known downstream target of TP53 and has been previously  
201 shown to exhibit increased expression within multiple contexts of cellular  
202 stress. *miR34a* asRNA has also been shown to be induced upon TP53  
203 activation in several global analyses of p53-regulated lncRNAs (Rashi-Elkeles  
204 et al. 2014, Hunten et al. 2015, Leveille et al. 2015, Ashouri et al. 2016, Kim et  
205 al. 2017). To confirm these results in our biological system, we treated  
206 HEK293t, embryonic kidney cells, and HCT116, colorectal cancer cells, with  
207 the DNA damaging agent doxorubicin to activate TP53. QPCR-mediated  
208 measurement of both *miR34a* HG and asRNA indicated that their expression  
209 levels were increased in response to doxorubicin treatment in both cell lines  
210 (**Fig. 2a**). To assess if it is in fact *TP53* that is responsible for the increase  
211 in *miR34a* asRNA expression upon DNA damage, we  
212 treated *TP53*<sup>+/+</sup> and *TP53*<sup>-/-</sup> HCT116 cells with increasing concentrations of  
213 doxorubicin and monitored the expression of both *miR34a* HG and asRNA.  
214 We observed a dose-dependent increase in both *miR34a* HG and asRNA  
215 expression levels with increasing amounts of doxorubicin, indicating that  
216 these two transcripts are co-regulated, although, this effect was largely  
217 abrogated in *TP53*<sup>-/-</sup> cells (**Fig. 2b**). These results indicate

218 that *TP53* activation increases *miR34a* asRNA expression upon the induction  
219 of DNA damage. Nevertheless, *TP53*<sup>-/-</sup> cells also showed a dose dependent  
220 increase in both *miR34a* HG and asRNA, indicating that additional factors,  
221 other than *TP53*, are capable of initiating an increase in expression of both of  
222 these transcripts upon DNA damage.

223

224



225 **Figure 2: TP53-mediated regulation of the *miR34a* locus.** **A)** Evaluating the effects of 24 hours of  
226 treatment with 200 ng/ml doxorubicin on *miR34a* asRNA and HG in HCT116 and HEK293  
227 cells.\* **B)** Monitoring *miR34a* HG and asRNA expression levels during 24 hours doxorubicin treatment  
228 in *TP53*<sup>+/+</sup> and *TP53*<sup>-/-</sup> HCT116 cells.\* **C)** Quantification of luciferase and renilla levels after  
229 transfection of HCT116 and HEK293T cells with the p1 construct (Figure 2 Supplement 2 contains a  
230 schematic representation of the p1 construct).\* **D)** HCT116 cells were co-transfected with the p1  
231 construct and shRNA renilla or shRNA control and subsequently treated with increasing doses of  
232 doxorubicin. 24 hours post-treatment, cells were harvested and renilla and luciferase levels were  
233 measured using QPCR. Resulting p-values from statistical testing are shown above the shRenilla  
234 samples which were compared to the shRNA control using the respective treatment condition.\*  
235 \*Individual points represent results from independent experiments and the gray shadow indicates the  
236 density of those points. Error bars show the 95% CI, black horizontal lines represent the mean, and p-  
237 values are shown over long horizontal lines indicating the comparison tested. All experiments in Figure  
238 2 were performed biological triplicate.

239

240 The head-to head orientation of *miR34a* HG and asRNA, suggests that  
241 transcription is initiated from a single promoter in a bi-directional manner. To  
242 investigate whether *miR34a* HG and asRNA are transcribed from the same  
243 promoter as divergent transcripts, we cloned the *miR34a* HG promoter,  
244 including the *TP53* binding site, into a luciferase/renilla dual reporter vector  
245 which we hereafter refer to as p1 (**Figure 2-Figure Supplement 1a-b**). Upon  
246 transfection of p1 into HCT116 and HEK293t cell lines we observed increases  
247 in both luciferase and renilla indicating that *miR34a* HG and asRNA  
248 expression can be regulated by a single promoter contained within the p1  
249 construct (**Fig. 2c**).

250

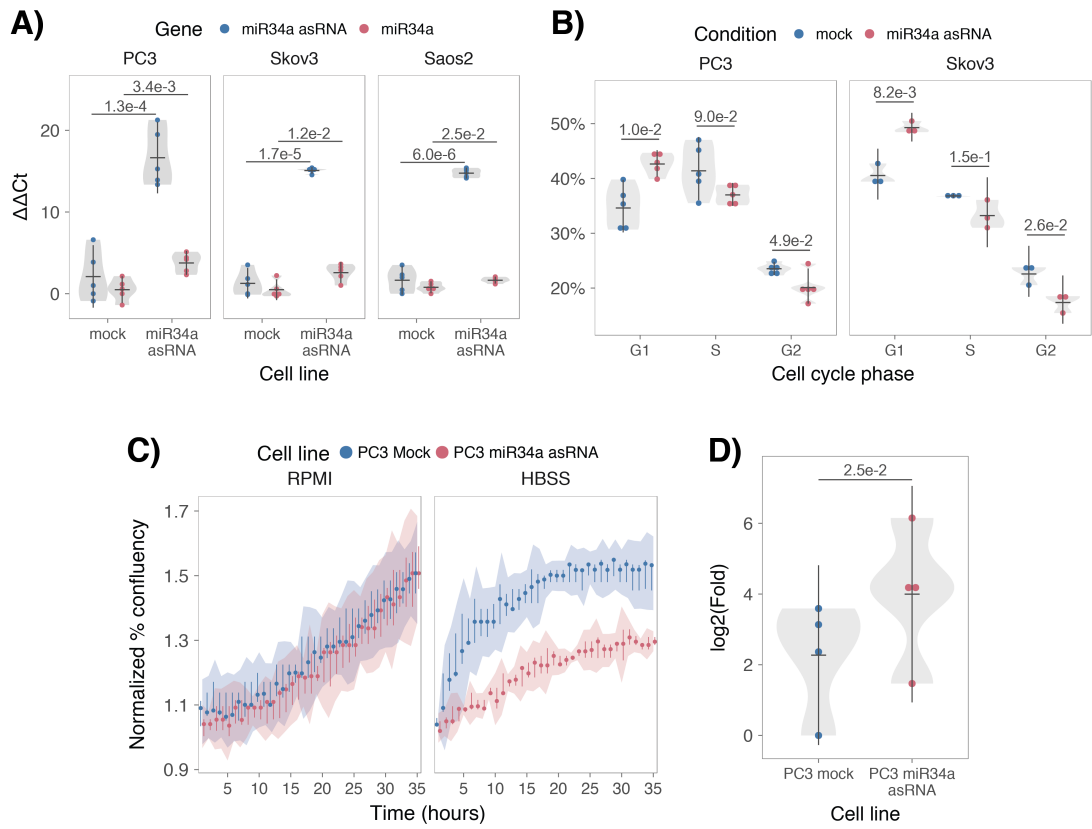
251 We hypothesized that *miR34a* asRNA may regulate *miR34a* HG levels and, in  
252 addition, that the overlapping regions of the sense and antisense transcripts  
253 may have a crucial role in mediating this regulation. Knock-down of  
254 endogenous *miR34a* asRNA is complicated by its various isoforms (**Figure 1-**  
255 **Figure Supplement 2c**). For this reason, we utilized the p1 construct to  
256 evaluate the regulatory role of the miR34a asRNA on miR34a HG.  
257 Accordingly, we first co-transfected the p1 construct, containing the  
258 overlapping region of the two transcripts, and two different short hairpin (sh)  
259 RNAs targeting renilla into HEK293T cells and subsequently measured  
260 luciferase and renilla expression. The results indicated that shRNA-mediated  
261 knock down of the p1-renilla transcript (corresponding to *miR34a* asRNA)  
262 caused p1-luciferase (corresponding to *miR34a* HG) levels to concomitantly  
263 decrease (**Figure 2-Figure Supplement 2**). These results indicate  
264 that *miR34a* asRNA positively regulates levels of *miR34a* HG and that the

265 transcriptional product of the *miR34a* asRNA within in the p1 construct  
266 promotes a miR34a response. To further support these conclusions and  
267 better understand the role of miR34a asRNA during TP53 activation, *TP53<sup>+/+</sup>*  
268 HCT116 cells were co-transfected with p1 and shRNA renilla (2.1) and  
269 subsequently treated with increasing doses of doxorubicin. Again, the results  
270 showed a concomitant reduction in luciferase levels upon knock-down of p1-  
271 renilla i.e. the *miR34a* asRNA corresponding segment of the p1 transcript  
272 (**Fig. 2d**). Furthermore, the results showed that in the absence of p1-renilla  
273 the expected induction of p1-luciferase in response to TP53 activation to DNA  
274 damage is abrogated. Collectively these results indicate that *miR34a* asRNA  
275 positively regulates *miR34a* expression and is crucial for an appropriate  
276 TP53-mediated *miR34a* response to DNA damage.

277

278 ***miR34a* asRNA regulates its host gene independently of TP53**  
279 Despite the fact that TP53 regulates *miR34a* HG and asRNA expression, our  
280 results indicated that other factors are also able to regulate this locus (**Fig.**  
281 **2b**). Utilizing a lentiviral system, we stably over-expressed the *miR34a* asRNA  
282 transcript in three *TP53*-null cell lines, PC3 (prostate cancer), Saos2  
283 (osteogenic sarcoma), and Skov3 (adenocarcinoma). We first analyzed the  
284 levels of *miR34a* asRNA in these stable over-expression cell lines, compared  
285 to HEK293T cells, which have high endogenous levels of *miR34a* asRNA,  
286 finding that, on average, the over-expression was approximately 30-fold  
287 higher in the over-expression cell lines than in HEK293t cells. Due to the fact  
288 that *miR34a* asRNA can be up-regulated ~30-fold in response to DNA  
289 damage (**Fig. 2b**), we deemed this over-expression level to correspond to

290 physiologically relevant levels in cells encountering a stress stimulus, such as  
291 DNA damage (**Figure 3-Figure Supplement 1**). Analysis of *miR34a* levels in  
292 the *miR34a* asRNA over-expressing cell lines showed that this over-  
293 expression resulted in a concomitant increase in the expression of *miR34a* in  
294 all three cell lines (**Fig. 3a**). These results indicate that, in the absence of  
295 *TP53*, *miR34a* expression may be rescued by increasing the levels  
296 of *miR34a* asRNA expression.



297

298 **Figure 3: miR34a asRNA positively regulates miR34a and its associated phenotypes.** **A)** QPCR-  
 299 mediated quantification of miR34a expression in cell lines stably over-  
 300 expressing miR34a asRNA.\* **B)** Cell cycle analysis comparing stably over-expressing miR34a asRNA  
 301 cells to the respective mock expressing cells.\* **C)** Analysis of cellular growth over time in miR34a  
 302 asRNA over-expressing PC3 cells. Points represent the median from 3 independent experiments, the  
 303 colored shadows indicate the 95% confidence interval, and vertical lines show the minimum and  
 304 maximum values obtained from the three biological replicates. **D)** Differential phosphorylated  
 305 polymerase II binding in miR34a asRNA over-expressing PC3 cells.\* \*Individual points represent  
 306 results from independent experiments and the gray shadow indicates the density of those points. Error  
 307 bars show the 95% CI, black horizontal lines represent the mean, and p-values are shown over long  
 308 horizontal lines indicating the comparison tested.  
 309

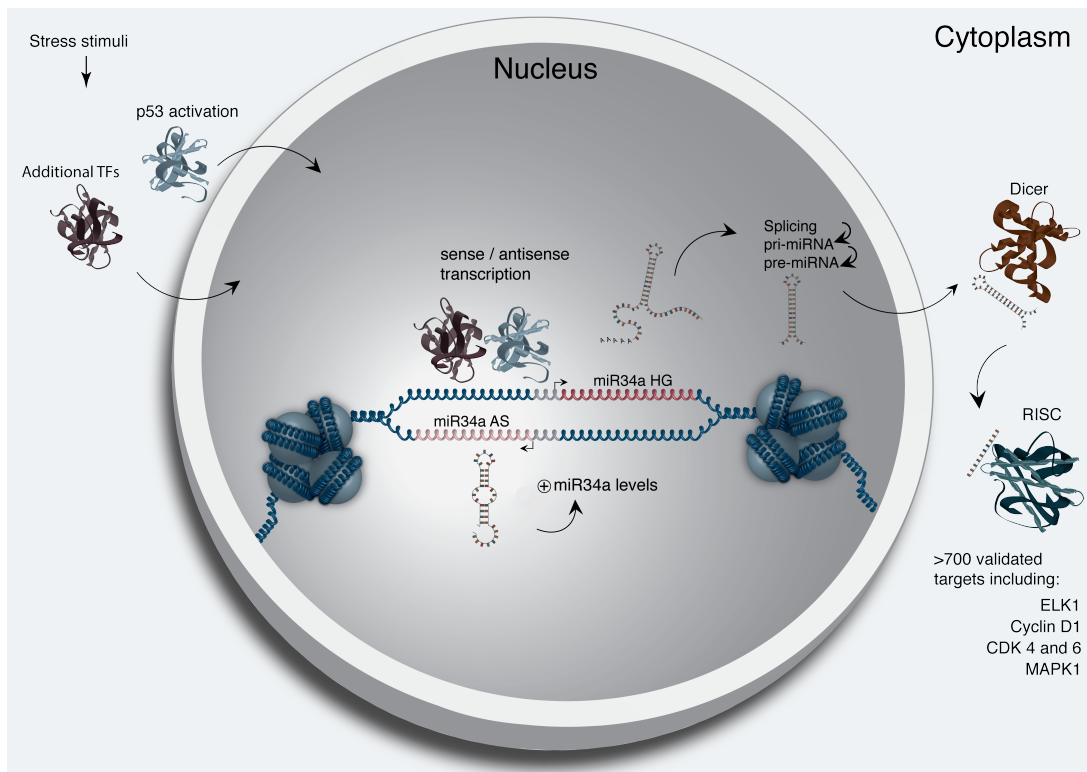
310 *miR34a* has been previously shown to regulate cell cycle progression, with  
311 *miR34a* induction causing G1 arrest (Raver-Shapira et al. 2007, Tarasov et al.  
312 2007). Cell cycle analysis via determination of DNA content showed a  
313 significant increase in G1 phase cells in the PC3 and Skov3 *miR34a* asRNA  
314 over-expressing cell lines, indicative of G1 arrest, as well as, a significant  
315 decrease of cells in G2 phase (**Fig. 3b**). *miR34a*'s effects on the cell cycle are  
316 mediated by its ability to target cell cycle regulators such as cyclin D1  
317 (*CCND1*) (Sun et al. 2008). We therefore sought to determine if  
318 the *miR34a* asRNA over-expressing cell lines exhibited effects on this  
319 known *miR34a* target. Quantification of both *CCND1* RNA expression (**Figure**  
320 **3-Figure Supplement 2a**) and protein levels (**Figure 3-Figure Supplement**  
321 **2b**) in the PC3 *miR34a* asRNA over-expressing cell line showed a significant  
322 decrease of *CCND1* levels compared to the mock control.

323  
324 *miR34a* is also a well known inhibitor of cellular growth via its ability to  
325 negatively regulate growth factor signaling. Furthermore, starvation has been  
326 shown to induce *miR34a* expression that down-regulates multiple targets that  
327 aid in the phosphorylation of pro-survival growth factors (Lal et al. 2011). We  
328 further interrogated the effects of *miR34a* asRNA over-expression by  
329 monitoring the growth of the cells in both normal and starvation conditions via  
330 confluency measurements over a 35-hour period. Under normal growth  
331 conditions there is a small but significant reduction ( $p = 3.0\text{e-}8$ ) in confluency  
332 in the *miR34a* asRNA over-expressing cell lines although, these effects on  
333 cell growth are drastically increased in starvation conditions ( $p = 9.5\text{e-}67$ ).  
334 This is in accordance with our previous results, and suggests

335 that *miR34a* asRNA-mediated increases in *miR34a* expression are crucial  
336 under conditions of stress and necessary for the initiation of an appropriate  
337 cellular response. In summary, we find that over-expression  
338 of *miR34a* asRNA is sufficient to increase *miR34a* expression and gives rise  
339 to known phenotypes observed with induction of *miR34a*.

340

341 Antisense RNAs have been reported to mediate their effects both via  
342 transcriptional and post-transcriptional mechanisms. Due to the fact that  
343 *miR34a* expression is undetected in wild type PC3 cells but, upon over-  
344 expression of *miR34a* asRNA, increases to detectable levels, we  
345 hypothesized that *miR34a* asRNA is capable of regulating *miR34a* expression  
346 via a transcriptional mechanism. To ascertain if this is actually the case, we  
347 performed chromatin immunoprecipitation (ChIP) for phosphorylated  
348 polymerase II (polII) at the *miR34a* HG promoter in both *miR34a* asRNA over-  
349 expressing and mock control cell lines. Our results indicated a clear increase  
350 in phosphorylated polII binding at the *miR34a* promoter upon *miR34a* asRNA  
351 over-expression indicating the ability of *miR34a* asRNA to regulate *miR34a*  
352 levels on a transcriptional level (**Fig. 3d**).



353

354 **Figure 4: A graphical summary of the proposed *miR34a* asRNA function.** Stress stimuli,  
 355 originating in the cytoplasm or nucleus, activates *TP53* as well as additional factors. These factors then  
 356 bind to the *miR34a* promoter and drive transcription of the sense and antisense strands. *miR34a* asRNA  
 357 serves to increase the levels of *miR34a* HG transcription via an unknown mechanism. *miR34a* HG  
 358 then, in turn, is then spliced, processed by the RNase III enzyme Drosha, and exported to the  
 359 cytoplasm. The *miR34a* pre-miRNA then binds to Dicer where the hair-pin loop is cleaved and  
 360 mature *miR34a* is formed. Binding of the mature *miR34a* miRNA to the RISC complex then allows it  
 361 to bind and repress its targets.

362 **Discussion**

363  
364 Multiple studies have previously shown asRNAs to be crucial for the  
365 appropriate regulation of cancer-associated protein-coding genes and that  
366 their dys-regulation can lead to perturbation of tumor suppressive and  
367 oncogenic pathways, as well as, cancer-related phenotypes (Yu et al. 2008,  
368 Yap et al. 2010, Serviss et al. 2014, Balbin et al. 2015). Here we show that  
369 asRNAs are also capable of regulating cancer-associated miRNAs resulting in  
370 similar consequences as protein-coding gene dys-regulation (**Fig. 4**).  
371 Interestingly, we show that, both in the presence and absence of  
372 *TP53*, *miR34a* asRNA provides an additional regulatory level and functions by  
373 mediating the increase of *miR34a* expression in both homeostasis and upon  
374 encountering multiple forms of cellular stress. Furthermore, we find that  
375 *miR34a* asRNA-mediated increases in *miR34a* expression levels are sufficient  
376 to drive the appropriate cellular responses to multiple forms of stress stimuli  
377 that are encountered (**Fig. 2d and Fig. 3c**). Previous studies have utilized  
378 various molecular methods to up regulate *miR34a* expression in a p53  
379 deficient background showing similar phenotypic outcomes but, to our  
380 knowledge, this is the first example of an endogenous mechanism by which  
381 this can be achieved (Liu et al. 2011, Ahn et al. 2012, Yang et al. 2012,  
382 Stahlhut et al. 2015, Wang et al. 2015).

383

384 In agreement with previous studies, we demonstrate that upon encountering  
385 various types of cellular stress, TP53 in concert with additional factors bind  
386 and initiate transcription at the *miR34a* locus, thus increasing the levels of  
387 *miR34a* and, in addition, *miR34a* asRNA. We hypothesize that *miR34a*

388 asRNA may provide positive feedback for *miR34a* expression whereby  
389 *miR34a* asRNA serves as a scaffold for the recruitment of additional factors  
390 that facilitate polymerase II-mediated transcription, thus, increasing the  
391 expression of *miR34a* and driving the cell towards a reduction in growth factor  
392 signaling, senescence, and eventually apoptosis. On the other hand, in cells  
393 without functional *TP53*, other factors, which typically act independently or in  
394 concert with *TP53*, may initiate transcription of the *miR34a* locus. We believe  
395 that *miR34a* asRNA could potentially be interacting directly with one of these  
396 additional factors and recruiting it to the *miR34a* locus in order to drive  
397 *miR34a* transcription. This is especially plausible due to head-to-head  
398 orientation of the *miR34a* HG and asRNA, causing sequence complementarity  
399 between the RNA and the promoter DNA. Previous reports have also  
400 illustrated the ability of asRNAs to form hybrid DNA:RNA R-loops and, thus,  
401 facilitate an open chromatin structure and the transcription of the sense gene  
402 (Boque-Sastre et al. 2015). The fact that the p1 construct only contains a  
403 small portion of the *miR34a* asRNA transcript indicates that this portion is  
404 sufficient to give rise to at least a partial *miR34a* inducing response and  
405 therefore, indicates that *miR34a* asRNA may be able to facilitate *miR34a*  
406 expression independent of additional factors (**Fig 2d, Figure 2-Figure**  
407 **Supplement 2a**). Nevertheless, further work will need to be performed to  
408 ascertain the mechanism that is utilized in the case of *miR34a* asRNA.

409

410 An antisense transcript arising from the *miR34a* locus, *Lnc34a*, has been  
411 previously reported to negatively regulate the expression of *miR34a* (Wang et  
412 al. 2016). Although the *Lnc34a* and *miR34a* asRNA transcripts share some

413 sequence similarity, we believe them to be separate RNAs that are,  
414 potentially, different isoforms of the same gene. We thoroughly address our  
415 reasons for these beliefs and give appropriate supporting evidence in  
416 (**Supplementary Document 1**). The fact that *Lnc34a* and *miR34a* asRNA  
417 would appear to have opposing roles in their regulation of *miR34a* further  
418 underlines the complexity of the regulation at this locus.

419

420 Clinical trials utilizing *miR34a* replacement therapy have previously been  
421 conducted but, disappointingly, were terminated after adverse side effects of  
422 an immunological nature were observed in several of the patients (Slabakova  
423 et al. 2017). Although it is not presently clear if these side effects were caused  
424 by *miR34a* or the liposomal carrier used to deliver the miRNA, the multitude of  
425 evidence indicating *miR34a*'s crucial role in oncogenesis still makes its  
426 therapeutic induction an interesting strategy for therapy and needs further  
427 investigation. In summary, our results indicate that *miR34a* asRNA is a vital  
428 player in the regulation of *miR34a* and is especially important in typical  
429 examples of cellular stress encountered in cancer. We believe the  
430 conclusions drawn in this study to be essential in the progress towards  
431 developing a better understanding of the regulation of cancer-associated  
432 miRNAs and, specifically, the tumor suppressor *miR34a*.

433

## 434 **Materials and Methods**

### 435 **Cell Culture**

436 All cell lines were cultured at 5% CO<sub>2</sub> and 37° C with HEK293T, Saos2, and  
437 Skov3 cells cultured in DMEM high glucose (GE Healthcare Life Sciences,

438 Hyclone, Amersham, UK, Cat# SH30081), HCT116 and U2OS cells in  
439 McCoy's 5a (ThermoFisher Scientific, Pittsburgh, MA, USA. Cat# SH30200),  
440 and PC3 cells in RPMI (GE Healthcare Life Sciences, Hyclone, Cat#  
441 SH3009602) and 2 mM L-glutamine (GE Healthcare Life Sciences, Hyclone,  
442 Cat# SH3003402). All growth mediums were supplemented with 10% heat-  
443 inactivated FBS (ThermoFisher Scientific, Gibco, Cat# 12657029) and 50  
444 µg/ml of streptomycin (ThermoFisher Scientific, Gibco, Cat# 15140122) and  
445 50 µg/ml of penicillin (ThermoFisher Scientific, Gibco, Cat# 15140122). All cell  
446 lines were purchased from ATCC, tested negative for mycoplasma, and their  
447 identity was verified via STR profiling.

448

#### 449 **Bioinformatics, Data Availability, and Statistical Testing**

450 The USCS genome browser (Kent et al. 2002) was utilized for the  
451 bioinformatic evaluation of antisense transcription utilizing the RefSeq  
452 (O'Leary et al. 2016) gene annotation track.

453

454 All raw experimental data, code used for analysis, and supplementary  
455 methods are available for review at ([Serviss 2017](#)) and are provided as an R  
456 package. All analysis took place using the R statistical programming language  
457 (Team 2017) using multiple external packages that are all documented in the  
458 package associated with the article (Wilkins , Chang 2014, Wickham 2014,  
459 Wickham 2016, Allaire et al. 2017, Arnold 2017, Wickham 2017, Wickham  
460 2017, Wickham 2017, Xiao 2017, Xie 2017). The package facilitates  
461 replication of the operating system and package versions used for the original  
462 analysis, reproduction of each individual figure and figure supplement  
463 included in the article, and easy review of the code used for all steps of the

464 analysis, from raw-data to figure.

465

466 The significance threshold (alpha) in this study was set to 0.05. Statistical  
467 testing was performed using a two sample Student's t-test unless otherwise  
468 specified.

469

## 470 **Coding Potential**

471 Protein-coding capacity was evaluated using the Coding-potential  
472 Assessment Tool (Wang et al. 2013) and Coding-potential Calculator (Kong et  
473 al. 2007) with default settings. Transcript sequences for use with Coding-  
474 potential Assessment Tool were downloaded from the UCSC genome  
475 browser using the Ensembl  
476 accessions: *HOTAIR* (ENST00000455246), *XIST* (ENST00000429829), β-  
477 actin (ENST00000331789), Tubulin (ENST00000427480),  
478 and *MYC* (ENST00000377970). Transcript sequences for use with Coding-  
479 potential Calculator were downloaded from the UCSC genome browser using  
480 the following IDs: *HOTAIR* (uc031qho.1), β-actin (uc003sqq.4).

481

## 482 **shRNAs**

483 shRNA-expressing constructs were cloned into the U6M2 construct using the  
484 BgIII and KpnI restriction sites as previously described (Amarzguioui et al.  
485 2005). shRNA constructs were transfected using Lipofectamine 2000 or 3000  
486 (ThermoFisher Scientific, Cat# 12566014 and L3000015). The sequences  
487 targeting renilla is as follows: shRenilla 1.1 (AAT ACA CCG CGC TAC TGG  
488 C), shRenilla 2.1 (TAA CGG GAT TTC ACG AGG C).

489 **Bi-directional Promoter Cloning**

490 The overlapping region (p1) corresponds with the sequence previously  
491 published as the TP53 binding site in (Raver-Shapira et al. 2007) which we  
492 synthesized, cloned into the pLucRluc construct (Polson et al. 2011) and  
493 sequenced to verify its identity.

494

495 **Promoter Activity**

496 Cells were co-transfected with the renilla/firefly bidirectional promoter  
497 construct (Polson et al. 2011) and GFP by using Lipofectamine 2000 (Life  
498 Technologies, Cat# 12566014). The expression of GFP and luminescence  
499 was measured 24 h post transfection by using the Dual-Glo Luciferase Assay  
500 System (Promega, Cat# E2920) and detected by the GloMax-Multi+ Detection  
501 System (Promega, Cat# SA3030). The expression of luminescence was  
502 normalized to GFP.

503

504 **Generation of U6-expressed miR34a AS Lentiviral Constructs**

505 The U6 promoter was amplified from the U6M2 cloning plasmid (Amarzguioui  
506 et al. 2005) and ligated into the Not1 restriction site of the pHIV7-IMPDH2  
507 vector (Turner et al. 2012). miR43a asRNA was PCR amplified and  
508 subsequently cloned into the Nhe1 and Pac1 restriction sites in the pHIV7-  
509 IMPDH2-U6 plasmid.

510

511 **Lentiviral Particle production, infection, and selection**

512 Lentivirus production was performed as previously described in (Turner et al.  
513 2012). Briefly, HEK293T cells were transfected with viral and expression

514 constructs using Lipofectamine 2000 (ThermoFisher Scientific, Cat#  
515 12566014), after which viral supernatants were harvested 48 and 72 hours  
516 post-transfection. Viral particles were concentrated using PEG-IT solution  
517 (Systems Biosciences, Palo Alto, CA, USA. Cat# LV825A-1) according to the  
518 manufacturer's recommendations. HEK293T cells were used for virus titration  
519 and GFP expression was evaluated 72hrs post-infection via flow cytometry  
520 (LSRII, BD Biosciences, San Jose, CA, USA) after which TU/ml was  
521 calculated.

522

523 Stable lines were generated by infecting cells with a multiplicity of infection of  
524 1 after which 1-2 µM mycophenolic acid (Merck, Kenilworth, NJ, USA. Cat#  
525 M5255) selection was initiated 48 hours post-infection. Cells were expanded  
526 as the selection process was monitored via flow cytometry analysis (LSRII,  
527 BD Biosciences) of GFP and selection was terminated once > 90% of the  
528 cells were GFP positive. Quantification of *miR34a* asRNA over-expression  
529 and *miR34a* was performed in biological quintuplet for all cell lines.

530

### 531 **Western Blotting**

532 Samples were lysed in 50 mM Tris-HCl (Sigma Aldrich, St. Louis, MO, USA.  
533 Cat# T2663), pH 7.4, 1% NP-40 (Sigma Aldrich, Cat# I8896), 150 mM NaCl  
534 (Sigma Aldrich, Cat# S5886), 1 mM EDTA (Promega, Madison, WI, USA.  
535 Cat# V4231), 1% glycerol (Sigma Aldrich, Cat# G5516), 100 µM vanadate  
536 (Sigma Aldrich, Cat# S6508), protease inhibitor cocktail (Roche Diagnostics,  
537 Basel, Switzerland, Cat# 004693159001) and PhosSTOP (Roche  
538 Diagnostics, Cat# 04906837001). Lysates were subjected to SDS-PAGE and

539 transferred to PVDF membranes. The proteins were detected by western blot  
540 analysis by using an enhanced chemiluminescence system (Western  
541 Lightning-ECL, PerkinElmer, Waltham, MA, USA. Cat# NEL103001EA).  
542 Antibodies used were specific for *CCND1* 1:1000 (Cell Signaling, Danvers,  
543 MA, USA. Cat# 2926), and β-actin 1:5000 (Sigma-Aldrich, Cat# A5441). All  
544 western blot quantifications were performed using ImageJ (Schneider et al.  
545 2012).

546

#### 547 **RNA Extraction and cDNA Synthesis**

548 For downstream SYBR green applications, RNA was extracted using the  
549 RNeasy mini kit (Qiagen, Venlo, Netherlands, Cat# 74106) and subsequently  
550 treated with DNase (Ambion Turbo DNA-free, ThermoFisher Scientific, Cat#  
551 AM1907). 500ng RNA was used for cDNA synthesis using MuMLV  
552 (ThermoFisher Scientific, Cat# 28025013) and a 1:1 mix of oligo(dT) and  
553 random nanomers.

554

555 For analysis of miRNA expression with Taqman, samples were isolated with  
556 TRIzol reagent (ThermoFisher Scientific, Cat# 15596018) and further  
557 processed with the miRNeasy kit (Qiagen, Cat# 74106). cDNA synthesis was  
558 performed using the TaqMan MicroRNA Reverse Transcription Kit  
559 (ThermoFisher Scientific, Cat# 4366597) using the corresponding oligos  
560 according to the manufacturer's recommendations.

561

#### 562 **QPCR and PCR**

563 PCR was performed using the KAPA2G Fast HotStart ReadyMix PCR Kit

564 (Kapa Biosystems, Wilmington, MA, USA, Cat# KK5601) with corresponding  
565 primers. QPCR was carried out using KAPA 2G SYBRGreen (Kapa  
566 Biosystems, Cat# KK4602) using the Applied Biosystems 7900HT machine  
567 with the cycling conditions: 95 °C for 3 min, 95 °C for 3 s, 60 °C for 30 s.

568

569 QPCR for miRNA expression analysis was performed according to the primer  
570 probe set manufacturers recommendations (ThermoFisher Scientific) and  
571 using the TaqMan Universal PCR Master Mix (ThermoFisher Scientific, Cat#  
572 4304437) with the same cycling scheme as above. Primer and probe sets for  
573 TaqMan were also purchased from ThermoFisher Scientific (Life  
574 Technologies at time of purchase, TaqMan® MicroRNA Assay, hsa-miR-34a,  
575 human, Cat# 4440887, Assay ID: 000426 and Control miRNA Assay, RNU48,  
576 human, Cat# 4440887, Assay ID: 001006).

577

578 The  $\Delta\Delta Ct$  method was used to quantify gene expression. All QPCR-based  
579 experiments were performed in at least technical duplicate. Primers for all  
580 PCR-based experiments are listed in **Supplementary Document 2** and  
581 arranged by figure.

582

### 583 **Cell Cycle Distribution**

584 Cells were washed in PBS and fixed in 4% paraformaldehyde at room  
585 temperature overnight. Paraformaldehyde was removed, and cells were re-  
586 suspended in 95% EtOH. The samples were then rehydrated in distilled  
587 water, stained with DAPI and analyzed by flow cytometry on a LSRII (BD  
588 Biosciences) machine. Resulting cell cycle phases were quantified using the

589 ModFit software (Verity Software House, Topsham, ME, USA). Experiments  
590 were performed in biological quadruplet (PC3) or triplicate (Skov3). The log<sub>2</sub>  
591 fraction of cell cycle phase was calculated for each replicate a two sample t-  
592 test was utilized for statistical testing.

593

594 **3' Rapid Amplification of cDNA Ends**

595 3'-RACE was performed as described as previously in (Johnsson et al. 2013).  
596 Briefly, U2OS cell RNA was polyA-tailed using yeast polyA polymerase  
597 (ThermoFisher Scientific, Cat# 74225Z25KU) after which cDNA was  
598 synthesized using oligo(dT) primers. Nested-PCR was performed first using a  
599 forward primer in miR34a asRNA exon 1 and a tailed oligo(dT) primer  
600 followed by a second PCR using an alternate miR34a asRNA exon 1 primer  
601 and a reverse primer binding to the tail of the previously used oligo(dT)  
602 primer. PCR products were gel purified and cloned the Strata Clone Kit  
603 (Agilent Technologies, Santa Clara, CA, USA. Cat# 240205), and sequenced.

604

605 **Chromatin Immunoprecipitation**

606 The ChIP was performed as previously described in (Johnsson et al. 2013)  
607 with the following modifications. Cells were crosslinked in 1% formaldehyde  
608 (Merck, Cat# 1040039025), quenched with 0.125M glycine (Sigma Aldrich,  
609 Cat# G7126), and lysed in cell lysis buffer comprised of: 5mM PIPES (Sigma  
610 Aldrich, Cat# 80635), 85mM KCL (Merck, Cat# 4936), 0.5% NP40 (Sigma  
611 Aldrich, Cat# I8896), protease inhibitor (Roche Diagnostics, Cat#  
612 004693159001). Samples were then sonicated in 50mM TRIS-HCL pH 8.0  
613 (Sigma Aldrich, MO, USA, Cat# T2663) 10mM EDTA (Promega, WI, USA,

614 Cat# V4231), 1% SDS (ThermoFisher Scientific, Cat# AM9822), and protease  
615 inhibitor (Roche Diagnostics, Cat# 004693159001) using a Bioruptor  
616 Sonicator (Diagenode, Denville, NJ, USA). Samples were incubated over  
617 night at 4°C with the *polII* antibody (Abcam, Cambridge, UK, Cat# ab5095)  
618 and subsequently pulled down with Salmon Sperm DNA/Protein A Agarose  
619 (Millipore, Cat# 16-157) beads. DNA was eluted in an elution buffer of 1%  
620 SDS (ThermoFisher Scientific, Cat# AM9822) 100mM NaHCO3 (Sigma  
621 Aldrich, Cat# 71631), followed by reverse crosslinking, RNaseA  
622 (ThermoFisher Scientific, Cat# 1692412) and protease K (New England  
623 Biolabs, Ipswich, MA, USA, Cat# P8107S) treatment. The DNA was eluted  
624 using Qiagen PCR purification kit (Cat# 28106) and quantified via QPCR.  
625 QPCR was performed in technical duplicate using the standard curve method  
626 and reported absolute values. The fraction of input was subsequently  
627 calculated using the mean of the technical replicates followed by calculating  
628 the fold over the control condition. Statistical testing was performed using 4  
629 biological replicates with the null hypothesis that the true log 2 fold change  
630 values were equal to zero.

631

### 632 **Confluency Analysis**

633 Cells were incubated in the Spark Multimode Microplate (Tecan, Männedorf,  
634 Switzerland) reader for 48 hours at 37°C with 5% CO<sub>2</sub> in a humidity chamber.  
635 Confluency was measured every hour using bright-field microscopy and the  
636 percentage of confluency was reported via the plate reader's inbuilt algorithm.  
637 Percentage of confluency was normalized to the control sample in each  
638 condition (shown in figure) and then ranked to move the data to a linear scale.

639 Using the mean of the technical duplicates in three biological replicates, the  
640 rank was then used to construct a linear model, of the dependency of the rank  
641 on the time and cell lines variables for each growth condition. Reported p-  
642 values are derived from the t-test, testing the null hypothesis that the  
643 coefficient estimate of the cell line variable is equal to 0.

644

#### 645 **Pharmacological Compounds**

646 Doxorubicin was purchased from Teva (Petah Tikva, Israel, cat. nr. 021361).

647

#### 648 **Cellular Localization Analysis**

649 Quantified RNAseq data from 11 cell lines from the GRCh38 assembly was  
650 downloaded from the ENCODE project database and quantifications for  
651 miR34a asRNA (ENSG00000234546), GAPDH (ENSG00000111640), and  
652 MALAT1 (ENSG00000251562) were extracted. Cell lines for which data was  
653 downloaded include: A549, GM12878, HeLa-S3, HepG2, HT1080, K562  
654 MCF-7, NCI-H460, SK-MEL-5, SK-N-DZ, SK-N-SH. Initial exploratory analysis  
655 revealed that several cell lines should be removed from the analysis due to a)  
656 a larger proportion of GAPDH in the nucleus than cytoplasm or b) variation of  
657 miR34a asRNA expression is too large to draw conclusions, or c) they have  
658 no or low (<6 TPM) miR34a asRNA expression. Furthermore, only  
659 polyadenylated libraries were used in the final analysis, due to the fact that  
660 the cellular compartment enrichment was improved in these samples. All  
661 analyzed genes are reported to be polyadenylated. In addition, only samples  
662 with 2 biological replicates were retained. For each cell type, gene, and  
663 biological replicate the fraction of transcripts per million (TPM) in each cellular

664 compartment was calculated as the fraction of TPM in the specific  
665 compartment by the total TPM. The mean and standard deviation for the  
666 fraction was subsequently calculated for each cell type and cellular  
667 compartment and this information was represented in the final figure.

668

## 669 **CAGE Analysis**

670 All available CAGE data from the ENCODE project (Consortium 2012) for 36  
671 cell lines was downloaded from the UCSC genome browser (Kent et al. 2002)  
672 for genome version hg19. Of these, 28 cell lines had CAGE transcription start  
673 sites (TSS) mapping to the plus strand of chromosome 1 and in regions  
674 corresponding to 200 base pairs upstream of the *lnc34a* start site (9241796 -  
675 200) and 200 base pairs upstream of the GENCODE  
676 annotated *miR34a* asRNA start site (9242263 + 200). These cell lines  
677 included: HFDPC, H1-hESC, HMEpC, HAoEC, HPIEpC, HSaVEC, GM12878,  
678 hMSC-BM, HUVEC, AG04450, hMSC-UC, IMR90, NHDF, SK-N-SH\_RA, BJ,  
679 HOB, HPC-PL, HAoAF, NHEK, HVMF, HWP, MCF-7, HepG2, hMSC-AT,  
680 NHEM.f\_M2, SkMC, NHEM\_M2, and HCH. In total 74 samples were included.  
681 17 samples were polyA-, 47 samples were polyA+, and 10 samples were total  
682 RNA. In addition, 34 samples were whole cell, 15 enriched for the cytosolic  
683 fraction, 15 enriched for the nucleolus, and 15 enriched for the nucleus. All  
684 CAGE transcription start sites were plotted and the RPKM of the individual  
685 reads was used to color each read to indicate their relative abundance. In  
686 cases where CAGE TSS spanned identical regions, the RPMKs of the regions  
687 were summed and represented as one CAGE TSS in the figure. In addition, a  
688 density plot shows the distribution of the CAGE reads in the specified

689 interval.

690

691 **Splice Junction Analysis**

692 All available whole cell (i.e. non-fractionated) spliced read data originating  
693 from the Cold Spring Harbor Lab in the ENCODE project (Consortium 2012)  
694 for 38 cell lines was downloaded from the UCSC genome browser (Kent et al.  
695 2002). Of these cell lines, 36 had spliced reads mapping to the plus strand of  
696 chromosome 1 and in the region between the *lnc34a* start (9241796) and  
697 transcription termination (9257102) site (note that *miR34a* asRNA resides  
698 totally within this region). Splice junctions from the following cell lines were  
699 included in the final figure: A549, Ag04450, Bj, CD20, CD34 mobilized,  
700 Gm12878, H1hesc, Haoaf, Haoec, Hch, Helas3, Hepg2, Hfdpc, Hmec,  
701 Hmepc, Hmscat, Hmscbm, Hmscuc, Hob, Hpcpl, Hpiepc, Hsavec, Hsmm,  
702 Huvec, Hvmf, Hwp, Imr90, Mcf7, Monocd14, Nhdf, Nhek, Nhemfm2,  
703 Nhemm2, Nhlf, Skmc, and Sknsh. All splice junctions were included in the  
704 figure and colored according to the number of reads corresponding to each. In  
705 cases where identical reads were detected multiple times, the read count was  
706 summed and represented as one read in the figure.

707

708 **TCGA Expression and Correlation Analysis**

709 Erik/Jimmy should probably take this.

710

711 **Acknowledgments**

712

713 **Competing Interests**

714

715 The authors declare no competing interests.

716

717 **Funding**

718  
719 This work has been supported by the Swedish Research Council [521-2012-2037],  
720 Swedish Cancer Society [150768], Cancer Research Foundations of Radiumhemmet  
721 [144063] and the Swedish Childhood Cancer Foundation [PR2015-0009].

722  
723  
724 **Figure Supplements**

725  
726 Figure 1-Supplement 1: TCAG expression levels and correlation analysis  
727 statistics.  
728  
729 Figure 1-Supplement 2: Molecular characteristics of miR34a asRNA.  
730  
731 Figure 2-Supplement 1: A schematic representation of the p1 construct.  
732  
733 Figure 2-Supplement 2: Evaluating the effects of miR34a asRNA down-  
734 regulation.  
735  
736 Figure 3-Supplement 1: Physiological relevance of miR34a asRNA  
737 overexpression.  
738  
739 Figure 3-Supplement 2: Effects of miR34a asRNA overexpression on cyclin  
740 D1.  
741  
742 Supplementary Document 1: Evaluating the relationship between miR34a  
743 asRNA and lnc34a.  
744  
745 Supplementary Document 2: A table of primers used in this study.

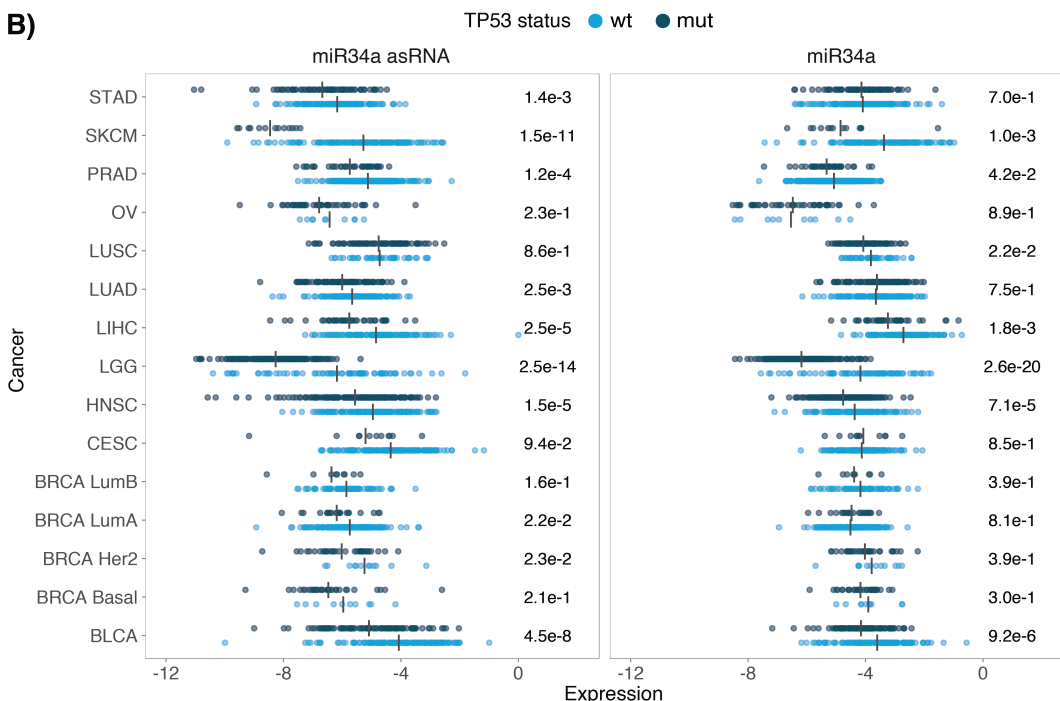
746 **Supplementary Figures**

747

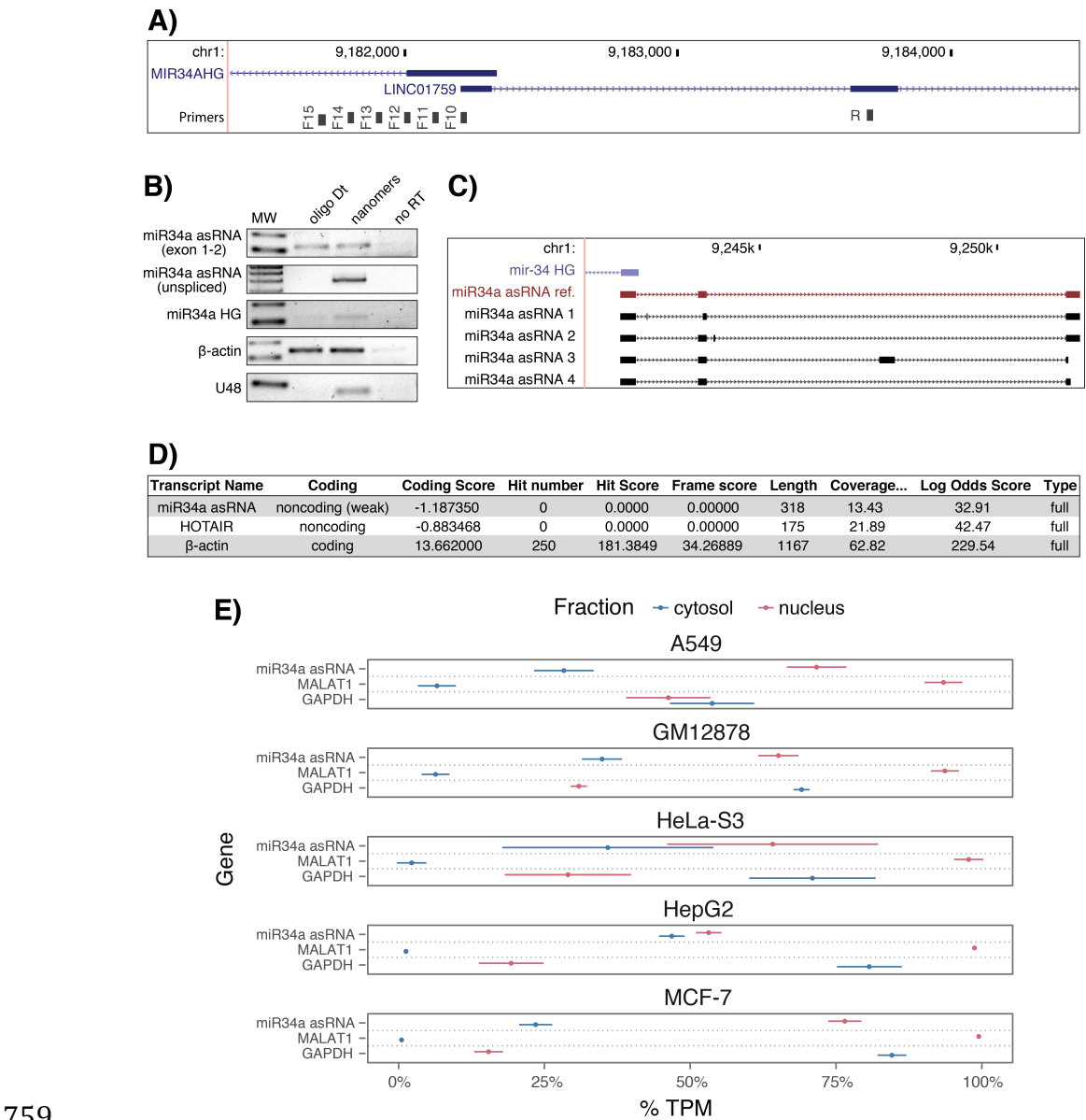
**A)**

cancer	all n	all rho	all p	TP53wt n	TP53wt rho	TP53wt p	TP53mut n	TP53mut rho	TP53mut p
ACC	10	5.52e-01	1.04e-01	10	5.52e-01	1.04e-01	NA	NA	NA
BLCA	228	5.15e-01	7.89e-17	134	4.53e-01	3.86e-08	94	4.27e-01	1.73e-05
BRCA Basal	42	5.74e-01	9.54e-05	10	6.24e-01	6.02e-02	32	5.74e-01	7.41e-04
BRCA Her2	44	1.47e-01	3.39e-01	12	2.24e-01	4.85e-01	32	6.82e-02	7.10e-01
BRCA LumA	199	3.41e-01	8.22e-07	177	3.43e-01	2.96e-06	22	4.86e-01	2.31e-02
BRCA LumB	70	1.71e-01	1.57e-01	61	1.48e-01	2.53e-01	9	1.67e-01	6.78e-01
CESC	156	1.39e-01	8.37e-02	145	1.60e-01	5.45e-02	11	-4.55e-02	9.03e-01
HNSC	313	5.37e-01	8.38e-25	123	6.08e-01	0.00e+00	190	4.47e-01	9.68e-11
KICH	5	6.00e-01	3.50e-01	5	6.00e-01	3.50e-01	NA	NA	NA
KIRC	142	3.49e-01	2.06e-05	141	3.37e-01	4.41e-05	NA	NA	NA
KIRP	167	4.51e-01	9.16e-10	163	4.48e-01	2.04e-09	4	8.00e-01	3.33e-01
LGG	271	6.33e-01	9.92e-32	76	7.28e-01	0.00e+00	195	3.87e-01	2.26e-08
LIHC	153	5.63e-01	3.64e-14	114	5.16e-01	4.18e-09	39	4.55e-01	3.95e-03
LUAD	234	2.82e-01	1.15e-05	128	3.61e-01	2.87e-05	106	2.27e-01	1.91e-02
LUSC	139	2.29e-01	6.74e-03	42	4.17e-02	7.93e-01	97	3.29e-01	9.91e-04
OV	56	2.33e-01	8.37e-02	10	8.42e-01	4.46e-03	46	1.46e-01	3.31e-01
PRAD	413	4.66e-01	1.33e-23	375	4.59e-01	6.13e-21	38	4.50e-01	4.58e-03
SKCM	165	6.48e-01	5.43e-21	152	6.10e-01	7.85e-17	13	4.34e-01	1.40e-01
STAD	225	3.72e-01	8.23e-09	145	3.67e-01	5.71e-06	80	4.20e-01	1.03e-04
THCA	469	4.58e-01	1.07e-25	467	4.62e-01	4.06e-26	NA	NA	NA

**B)**

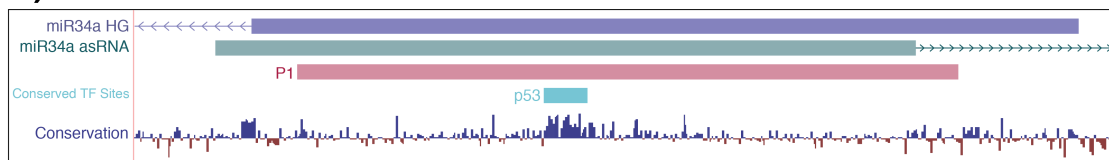


748  
749  
750 **Figure 1 Supplement 1: TCAG expression levels and correlation analysis statistics. A)** Spearman's  
751 rho and p-values (p) from the correlation analysis investigating the correlation between miR34a and  
752 miR34a asRNA expression in TP53 wild type (wt) and mutated (mut) samples within TCGA cancer  
753 types. **B)** Expression levels of miR34a and miR34a asRNA in TP53 wt and nonsynonymous mutation  
754 samples. Bladder Urothelial Carcinoma (BLCA), Breast invasive carcinoma (BRCA), Head and Neck  
755 squamous cell carcinoma (HNSC), Lower Grade Glioma (LGG), Liver hepatocellular carcinoma  
756 (LIHC), Lung adenocarcinoma (LUAD), Lung squamous cell carcinoma (LUSC), Ovarian serous  
757 cystadenocarcinoma (OV), Prostate adenocarcinoma (PRAD), Skin Cutaneous Melanoma (SKCM),  
758 Stomach adenocarcinoma (STAD).



759  
760  
761 **Figure 1 Supplement 2: Molecular characteristics of miR34a asRNA.** A) A schematic  
762 representation of the primer placement in the primer walk assay. B) Polyadenylation status of spliced  
763 and unspliced miR34a asRNA in HEK293T cells. C) Sequencing results from the analysis  
764 of *miR34a* asRNA isoforms in U2OS cells. *miR34a* AS ref. refers to the full length transcript as  
765 defined by the 3'-RACE and primer walk assay. D) Analysis of coding potential of the *miR34a* asRNA  
766 transcript using the Coding-potential Calculator. E) RNAseq data from five fractionated cell lines in  
767 the ENCODE project showing the percentage of transcripts per million (TPM) for miR34a asRNA.  
768 MALAT1 (nuclear localization) and GAPDH (cytoplasmic localization) are included as fractionation  
769 controls. Points represent the mean and horizontal lines represent the standard deviation from two  
770 biological replicates.  
771

**A)**

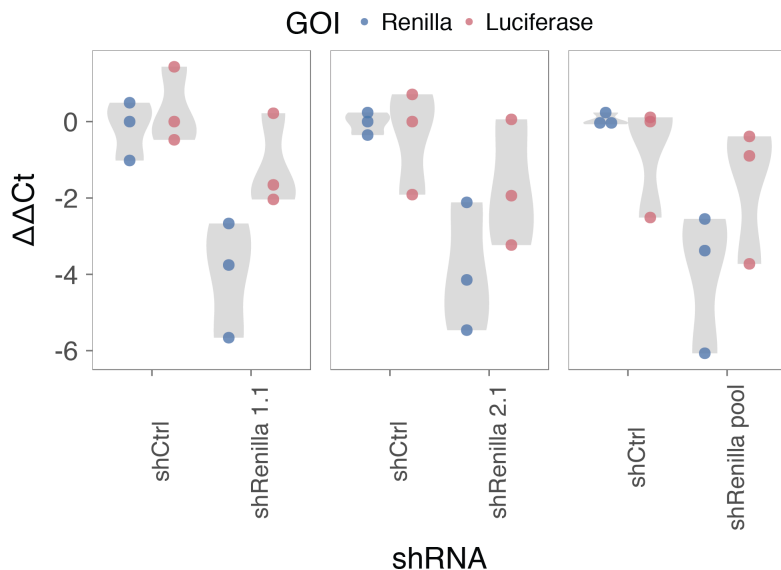


**B)**



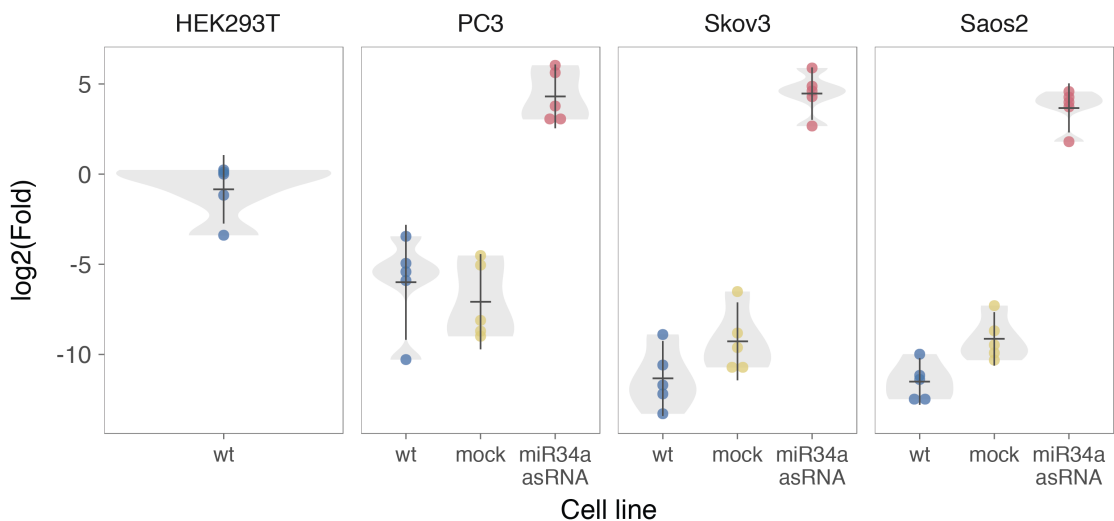
772  
773  
774  
775  
776  
777

**Figure 2 Supplement 1: A schematic representation of the p1 construct. A)** A UCSC genome browser illustration indicating the location of the promoter region cloned into the p1 construct including the conserved *TP53*-binding site. **B)** A representative picture of the p1 construct including forward (F) and reverse (R) primer locations and the renilla shRNA targeting site.



778  
779  
780  
781  
782  
783  
784

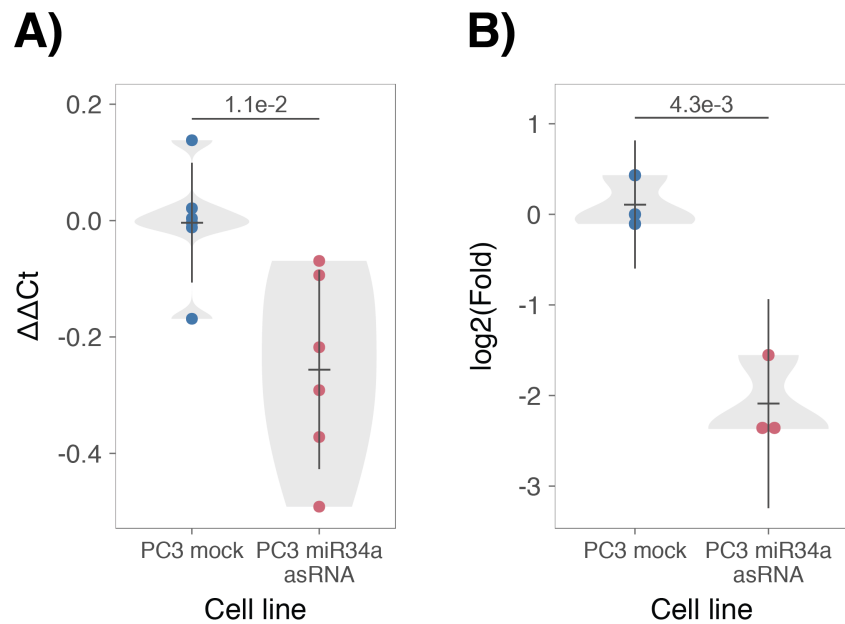
**Figure 2 Supplement 2: Evaluating the effects of miR34a asRNA down-regulation.** HEK293T cells were co-transfected with the P1 construct and either shRenilla or shControl. Renilla and luciferase levels were measured with Q-PCR 48 hours after transfection. Individual points represent independent experiments with the gray shadow indicating the density of the points. The experiment was performed in biological triplicate.



785

786

787 **Figure 3 Supplement 1: Physiological relevance of miR34a asRNA overexpression.** Comparison  
788 of *miR34a* asRNA expression in HEK293T cells (high endogenous *miR34a* asRNA), and the wild-type  
789 (wt), mock, and *miR34a* asRNA over-expressing stable cell lines.



790  
791  
792  
793  
794

**Figure 3 Supplement 2: Effects of miR34a asRNA overexpression on cyclin D1.** CCND1 expression (A) and western blot quantification of protein levels (B) in *miR34a* asRNA over-expressing PC3 stable cell lines. Experiments were performed in biological sextuplets (A) or triplicates (B).

795      **References**  
796

- 797      Agostini, M., P. Tucci, R. Killick, E. Candi, B. S. Sayan, P. Rivetti di Val Cervo, P.  
798      Nicotera, F. McKeon, R. A. Knight, T. W. Mak and G. Melino (2011). "Neuronal  
799      differentiation by TAp73 is mediated by microRNA-34a regulation of synaptic  
800      protein targets." *Proc Natl Acad Sci U S A* **108**(52): 21093-21098. DOI:  
801      10.1073/pnas.1112061109  
802
- 803      Ahn, Y. H., D. L. Gibbons, D. Chakravarti, C. J. Creighton, Z. H. Rizvi, H. P. Adams, A.  
804      Pertsemlidis, P. A. Gregory, J. A. Wright, G. J. Goodall, E. R. Flores and J. M. Kurie  
805      (2012). "ZEB1 drives prometastatic actin cytoskeletal remodeling by  
806      downregulating miR-34a expression." *J Clin Invest* **122**(9): 3170-3183. DOI:  
807      10.1172/JCI63608  
808
- 809      Allaire, J., Y. Xie, J. McPherson, J. Luraschi, K. Ushey, A. Atkins, H. Wickham, J.  
810      Cheng and W. Chang (2017). rmarkdown: Dynamic Documents for R. R package  
811      version 1.8. <https://CRAN.R-project.org/package=rmarkdown>  
812
- 813      Amarzguioui, M., J. J. Rossi and D. Kim (2005). "Approaches for chemically  
814      synthesized siRNA and vector-mediated RNAi." *FEBS Lett* **579**(26): 5974-5981.  
815      DOI: 10.1016/j.febslet.2005.08.070  
816
- 817      Arnold, J. B. (2017). ggthemes: Extra Themes, Scales and Geoms for 'ggplot2'. R  
818      package version 3.4.0. <https://CRAN.R-project.org/package=ggthemes>  
819
- 820      Ashouri, A., V. I. Sayin, J. Van den Eynden, S. X. Singh, T. Papagiannakopoulos and  
821      E. Larsson (2016). "Pan-cancer transcriptomic analysis associates long non-  
822      coding RNAs with key mutational driver events." *Nature Communications* **7**:  
823      13197. DOI: 10.1038/ncomms13197  
824
- 825      Balbin, O. A., R. Malik, S. M. Dhanasekaran, J. R. Prensner, X. Cao, Y. M. Wu, D.  
826      Robinson, R. Wang, G. Chen, D. G. Beer, A. I. Nesvizhskii and A. M. Chinnaian  
827      (2015). "The landscape of antisense gene expression in human cancers." *Genome  
828      Res* **25**(7): 1068-1079. DOI: 10.1101/gr.180596.114  
829
- 830      Boque-Sastre, R., M. Soler, C. Oliveira-Mateos, A. Portela, C. Moutinho, S. Sayols, A.  
831      Villanueva, M. Esteller and S. Guil (2015). "Head-to-head antisense transcription  
832      and R-loop formation promotes transcriptional activation." *Proc Natl Acad Sci U  
833      SA* **112**(18): 5785-5790. DOI: 10.1073/pnas.1421197112  
834
- 835      Chang, T. C., D. Yu, Y. S. Lee, E. A. Wentzel, D. E. Arking, K. M. West, C. V. Dang, A.  
836      Thomas-Tikhonenko and J. T. Mendell (2008). "Widespread microRNA  
837      repression by Myc contributes to tumorigenesis." *Nat Genet* **40**(1): 43-50. DOI:  
838      10.1038/ng.2007.30  
839
- 840      Chang, W. (2014). extrafont: Tools for using fonts. R package version 0.17.  
841      <https://CRAN.R-project.org/package=extrafont>  
842

- 843 Chen, J., M. Sun, W. J. Kent, X. Huang, H. Xie, W. Wang, G. Zhou, R. Z. Shi and J. D.  
844 Rowley (2004). "Over 20% of human transcripts might form sense-antisense  
845 pairs." *Nucleic Acids Res* **32**(16): 4812-4820. DOI: 10.1093/nar/gkh818
- 846
- 847 Cheng, J., L. Zhou, Q. F. Xie, H. Y. Xie, X. Y. Wei, F. Gao, C. Y. Xing, X. Xu, L. J. Li and S.  
848 S. Zheng (2010). "The impact of miR-34a on protein output in hepatocellular  
849 carcinoma HepG2 cells." *Proteomics* **10**(8): 1557-1572. DOI:  
850 10.1002/pmic.200900646
- 851
- 852 Chim, C. S., K. Y. Wong, Y. Qi, F. Loong, W. L. Lam, L. G. Wong, D. Y. Jin, J. F. Costello  
853 and R. Liang (2010). "Epigenetic inactivation of the miR-34a in hematological  
854 malignancies." *Carcinogenesis* **31**(4): 745-750. DOI: 10.1093/carcin/bgq033
- 855
- 856 Cole, K. A., E. F. Attiyeh, Y. P. Mosse, M. J. Laquaglia, S. J. Diskin, G. M. Brodeur and  
857 J. M. Maris (2008). "A functional screen identifies miR-34a as a candidate  
858 neuroblastoma tumor suppressor gene." *Mol Cancer Res* **6**(5): 735-742. DOI:  
859 10.1158/1541-7786.MCR-07-2102
- 860
- 861 Conley, A. B. and I. K. Jordan (2012). "Epigenetic regulation of human cis-natural  
862 antisense transcripts." *Nucleic Acids Res* **40**(4): 1438-1445. DOI:  
863 10.1093/nar/gkr1010
- 864
- 865 Consortium, E. P. (2012). "An integrated encyclopedia of DNA elements in the  
866 human genome." *Nature* **489**(7414): 57-74. DOI: 10.1038/nature11247
- 867
- 868 Ding, N., H. Wu, T. Tao and E. Peng (2017). "NEAT1 regulates cell proliferation  
869 and apoptosis of ovarian cancer by miR-34a-5p/BCL2." *Onco Targets Ther* **10**:  
870 4905-4915. DOI: 10.2147/OTT.S142446
- 871
- 872 Djebali, S., C. A. Davis, A. Merkel, A. Dobin, T. Lassmann, A. Mortazavi, A. Tanzer, J.  
873 Lagarde, W. Lin, F. Schlesinger, C. Xue, G. K. Marinov, J. Khatun, B. A. Williams, C.  
874 Zaleski, J. Rozowsky, M. Roder, F. Kokocinski, R. F. Abdelhamid, T. Alioto, I.  
875 Antoshechkin, M. T. Baer, N. S. Bar, P. Batut, K. Bell, I. Bell, S. Chakrabortty, X.  
876 Chen, J. Chrast, J. Curado, T. Derrien, J. Drenkow, E. Dumais, J. Dumais, R.  
877 Duttagupta, E. Falconnet, M. Fastuca, K. Fejes-Toth, P. Ferreira, S. Foissac, M. J.  
878 Fullwood, H. Gao, D. Gonzalez, A. Gordon, H. Gunawardena, C. Howald, S. Jha, R.  
879 Johnson, P. Kapranov, B. King, C. Kingswood, O. J. Luo, E. Park, K. Persaud, J. B.  
880 Preall, P. Ribeca, B. Risk, D. Robyr, M. Sammeth, L. Schaffer, L. H. See, A. Shahab, J.  
881 Skancke, A. M. Suzuki, H. Takahashi, H. Tilgner, D. Trout, N. Walters, H. Wang, J.  
882 Wrobel, Y. Yu, X. Ruan, Y. Hayashizaki, J. Harrow, M. Gerstein, T. Hubbard, A.  
883 Reymond, S. E. Antonarakis, G. Hannon, M. C. Giddings, Y. Ruan, B. Wold, P.  
884 Carninci, R. Guigo and T. R. Gingeras (2012). "Landscape of transcription in  
885 human cells." *Nature* **489**(7414): 101-108. DOI: 10.1038/nature11233
- 886
- 887 Gallardo, E., A. Navarro, N. Vinolas, R. M. Marrades, T. Diaz, B. Gel, A. Quera, E.  
888 Bandres, J. Garcia-Foncillas, J. Ramirez and M. Monzo (2009). "miR-34a as a  
889 prognostic marker of relapse in surgically resected non-small-cell lung cancer."  
890 *Carcinogenesis* **30**(11): 1903-1909. DOI: 10.1093/carcin/bgp219
- 891

- 892 Hunten, S., M. Kaller, F. Drepper, S. Oeljeklaus, T. Bonfert, F. Erhard, A. Dueck, N.  
893 Eichner, C. C. Friedel, G. Meister, R. Zimmer, B. Warscheid and H. Hermeking  
894 (2015). "p53-Regulated Networks of Protein, mRNA, miRNA, and lncRNA  
895 Expression Revealed by Integrated Pulsed Stable Isotope Labeling With Amino  
896 Acids in Cell Culture (pSILAC) and Next Generation Sequencing (NGS) Analyses."  
897 Mol Cell Proteomics **14**(10): 2609-2629. DOI: 10.1074/mcp.M115.050237
- 898
- 899 International Human Genome Sequencing, C. (2004). "Finishing the euchromatic  
900 sequence of the human genome." Nature **431**(7011): 931-945. DOI:  
901 10.1038/nature03001
- 902
- 903 Johnsson, P., A. Ackley, L. Vidarsdottir, W. O. Lui, M. Corcoran, D. Grander and K.  
904 V. Morris (2013). "A pseudogene long-noncoding-RNA network regulates PTEN  
905 transcription and translation in human cells." Nat Struct Mol Biol **20**(4): 440-  
906 446. DOI: 10.1038/nsmb.2516
- 907
- 908 Katayama, S., Y. Tomaru, T. Kasukawa, K. Waki, M. Nakanishi, M. Nakamura, H.  
909 Nishida, C. C. Yap, M. Suzuki, J. Kawai, H. Suzuki, P. Carninci, Y. Hayashizaki, C.  
910 Wells, M. Frith, T. Ravasi, K. C. Pang, J. Hallinan, J. Mattick, D. A. Hume, L. Lipovich,  
911 S. Batalov, P. G. Engstrom, Y. Mizuno, M. A. Faghihi, A. Sandelin, A. M. Chalk, S.  
912 Mottagui-Tabar, Z. Liang, B. Lenhard, C. Wahlestedt, R. G. E. R. Group, G. Genome  
913 Science and F. Consortium (2005). "Antisense transcription in the mammalian  
914 transcriptome." Science **309**(5740): 1564-1566. DOI: 10.1126/science.1112009
- 915
- 916 Kent, W. J., C. W. Sugnet, T. S. Furey, K. M. Roskin, T. H. Pringle, A. M. Zahler and D.  
917 Haussler (2002). "The human genome browser at UCSC." Genome Res **12**(6):  
918 996-1006. DOI: 10.1101/gr.229102. Article published online before print in May  
919 2002
- 920
- 921 Kim, K. H., H. J. Kim and T. R. Lee (2017). "Epidermal long non-coding RNAs are  
922 regulated by ultraviolet irradiation." Gene **637**: 196-202. DOI:  
923 10.1016/j.gene.2017.09.043
- 924
- 925 Kong, L., Y. Zhang, Z. Q. Ye, X. Q. Liu, S. Q. Zhao, L. Wei and G. Gao (2007). "CPC:  
926 assess the protein-coding potential of transcripts using sequence features and  
927 support vector machine." Nucleic Acids Res **35**(Web Server issue): W345-349.  
928 DOI: 10.1093/nar/gkm391
- 929
- 930 Lal, A., M. P. Thomas, G. Altschuler, F. Navarro, E. O'Day, X. L. Li, C. Concepcion, Y.  
931 C. Han, J. Thiery, D. K. Rajani, A. Deutsch, O. Hofmann, A. Ventura, W. Hide and J.  
932 Lieberman (2011). "Capture of microRNA-bound mRNAs identifies the tumor  
933 suppressor miR-34a as a regulator of growth factor signaling." PLoS Genet **7**(11):  
934 e1002363. DOI: 10.1371/journal.pgen.1002363
- 935
- 936 Leveille, N., C. A. Melo, K. Rooijers, A. Diaz-Lagares, S. A. Melo, G. Korkmaz, R.  
937 Lopes, F. Akbari Moqadam, A. R. Maia, P. J. Wijchers, G. Geeven, M. L. den Boer, R.  
938 Kalluri, W. de Laat, M. Esteller and R. Agami (2015). "Genome-wide profiling of  
939 p53-regulated enhancer RNAs uncovers a subset of enhancers controlled by a  
940 lncRNA." Nature Communications **6**: 6520. DOI: 10.1038/ncomms7520

941  
942 Liu, C., K. Kelnar, B. Liu, X. Chen, T. Calhoun-Davis, H. Li, L. Patrawala, H. Yan, C.  
943 Jeter, S. Honorio, J. F. Wiggins, A. G. Bader, R. Fagin, D. Brown and D. G. Tang  
944 (2011). "The microRNA miR-34a inhibits prostate cancer stem cells and  
945 metastasis by directly repressing CD44." *Nat Med* **17**(2): 211-215. DOI:  
946 10.1038/nm.2284  
947  
948 Memczak, S., M. Jens, A. Elefsinioti, F. Torti, J. Krueger, A. Rybak, L. Maier, S. D.  
949 Mackowiak, L. H. Gregersen, M. Munschauer, A. Loewer, U. Ziebold, M.  
950 Landthaler, C. Kocks, F. le Noble and N. Rajewsky (2013). "Circular RNAs are a  
951 large class of animal RNAs with regulatory potency." *Nature* **495**(7441): 333-  
952 338. DOI: 10.1038/nature11928  
953  
954 O'Leary, N. A., M. W. Wright, J. R. Brister, S. Ciufo, D. Haddad, R. McVeigh, B.  
955 Rajput, B. Robbertse, B. Smith-White, D. Ako-Adjei, A. Astashyn, A. Badretdin, Y.  
956 Bao, O. Blinkova, V. Brover, V. Chetvernin, J. Choi, E. Cox, O. Ermolaeva, C. M.  
957 Farrell, T. Goldfarb, T. Gupta, D. Haft, E. Hatcher, W. Hlavina, V. S. Joardar, V. K.  
958 Kodali, W. Li, D. Maglott, P. Masterson, K. M. McGarvey, M. R. Murphy, K. O'Neill,  
959 S. Pujar, S. H. Rangwala, D. Rausch, L. D. Riddick, C. Schoch, A. Shkeda, S. S. Storz,  
960 H. Sun, F. Thibaud-Nissen, I. Tolstoy, R. E. Tully, A. R. Vatsan, C. Wallin, D. Webb,  
961 W. Wu, M. J. Landrum, A. Kimchi, T. Tatusova, M. DiCuccio, P. Kitts, T. D. Murphy  
962 and K. D. Pruitt (2016). "Reference sequence (RefSeq) database at NCBI: current  
963 status, taxonomic expansion, and functional annotation." *Nucleic Acids Res*  
964 **44**(D1): D733-745. DOI: 10.1093/nar/gkv1189  
965  
966 Ozsolak, F., P. Kapranov, S. Foissac, S. W. Kim, E. Fishilevich, A. P. Monaghan, B.  
967 John and P. M. Milos (2010). "Comprehensive polyadenylation site maps in yeast  
968 and human reveal pervasive alternative polyadenylation." *Cell* **143**(6): 1018-  
969 1029. DOI: 10.1016/j.cell.2010.11.020  
970  
971 Polson, A., E. Durrett and D. Reisman (2011). "A bidirectional promoter reporter  
972 vector for the analysis of the p53/WDR79 dual regulatory element." *Plasmid*  
973 **66**(3): 169-179. DOI: 10.1016/j.plasmid.2011.08.004  
974  
975 Rashi-Elkeles, S., H. J. Warnatz, R. Elkon, A. Kupershtein, Y. Chobod, A. Paz, V.  
976 Amstislavskiy, M. Sultan, H. Safer, W. Nietfeld, H. Lehrach, R. Shamir, M. L. Yaspo  
977 and Y. Shiloh (2014). "Parallel profiling of the transcriptome, cistrome, and  
978 epigenome in the cellular response to ionizing radiation." *Sci Signal* **7**(325): rs3.  
979 DOI: 10.1126/scisignal.2005032  
980  
981 Raver-Shapira, N., E. Marciano, E. Meiri, Y. Spector, N. Rosenfeld, N. Moskovits, Z.  
982 Bentwich and M. Oren (2007). "Transcriptional activation of miR-34a  
983 contributes to p53-mediated apoptosis." *Mol Cell* **26**(5): 731-743. DOI:  
984 10.1016/j.molcel.2007.05.017  
985  
986 Rinn, J. L., M. Kertesz, J. K. Wang, S. L. Squazzo, X. Xu, S. A. Brugmann, L. H.  
987 Goodnough, J. A. Helms, P. J. Farnham, E. Segal and H. Y. Chang (2007).  
988 "Functional demarcation of active and silent chromatin domains in human HOX

989 loci by noncoding RNAs." *Cell* **129**(7): 1311-1323. DOI:  
990 10.1016/j.cell.2007.05.022  
991  
992 Rokavec, M., M. G. Oner, H. Li, R. Jackstadt, L. Jiang, D. Lodygin, M. Kaller, D. Horst,  
993 P. K. Ziegler, S. Schwitalla, J. Slotta-Huspenina, F. G. Bader, F. R. Greten and H.  
994 Hermeking (2015). "Corrigendum. IL-6R/STAT3/miR-34a feedback loop  
995 promotes EMT-mediated colorectal cancer invasion and metastasis." *J Clin Invest*  
996 **125**(3): 1362. DOI: 10.1172/JCI81340  
997  
998 Schneider, C. A., W. S. Rasband and K. W. Eliceiri (2012). "NIH Image to ImageJ:  
999 25 years of image analysis." *Nat Methods* **9**(7): 671-675.  
1000  
1001 Serviss, J. T. (2017). miR34AasRNaproject.  
1002 [https://github.com/GranderLab/miR34a\\_asRNA\\_project](https://github.com/GranderLab/miR34a_asRNA_project)  
1003  
1004 Serviss, J. T., P. Johnsson and D. Grander (2014). "An emerging role for long non-  
1005 coding RNAs in cancer metastasis." *Front Genet* **5**: 234. DOI:  
1006 10.3389/fgene.2014.00234  
1007  
1008 Slabakova, E., Z. Culig, J. Remsik and K. Soucek (2017). "Alternative mechanisms  
1009 of miR-34a regulation in cancer." *Cell Death Dis* **8**(10): e3100. DOI:  
1010 10.1038/cddis.2017.495  
1011  
1012 Stahlhut, C. and F. J. Slack (2015). "Combinatorial Action of MicroRNAs let-7 and  
1013 miR-34 Effectively Synergizes with Erlotinib to Suppress Non-small Cell Lung  
1014 Cancer Cell Proliferation." *Cell Cycle* **14**(13): 2171-2180. DOI:  
1015 10.1080/15384101.2014.1003008  
1016  
1017 Su, X., D. Chakravarti, M. S. Cho, L. Liu, Y. J. Gi, Y. L. Lin, M. L. Leung, A. El-Naggar,  
1018 C. J. Creighton, M. B. Suraokar, I. Wistuba and E. R. Flores (2010). "TAp63  
1019 suppresses metastasis through coordinate regulation of Dicer and miRNAs."  
1020 *Nature* **467**(7318): 986-990. DOI: 10.1038/nature09459  
1021  
1022 Sun, F., H. Fu, Q. Liu, Y. Tie, J. Zhu, R. Xing, Z. Sun and X. Zheng (2008).  
1023 "Downregulation of CCND1 and CDK6 by miR-34a induces cell cycle arrest."  
1024 *FEBS Lett* **582**(10): 1564-1568. DOI: 10.1016/j.febslet.2008.03.057  
1025  
1026 Tarasov, V., P. Jung, B. Verdoodt, D. Lodygin, A. Epanchintsev, A. Menssen, G.  
1027 Meister and H. Hermeking (2007). "Differential regulation of microRNAs by p53  
1028 revealed by massively parallel sequencing: miR-34a is a p53 target that induces  
1029 apoptosis and G1-arrest." *Cell Cycle* **6**(13): 1586-1593. DOI:  
1030 10.4161/cc.6.13.4436  
1031  
1032 Team, R. C. (2017). "R: A Language and Environment for Statistical Computing."  
1033 from <https://www.R-project.org/>.  
1034  
1035 Turner, A. M., A. M. Ackley, M. A. Matrone and K. V. Morris (2012).  
1036 "Characterization of an HIV-targeted transcriptional gene-silencing RNA in  
1037 primary cells." *Hum Gene Ther* **23**(5): 473-483. DOI: 10.1089/hum.2011.165

1038  
1039 Vogt, M., J. Mundig, M. Gruner, S. T. Liffers, B. Verdoodt, J. Hauk, L.  
1040 Steinstraesser, A. Tannapfel and H. Hermeking (2011). "Frequent concomitant  
1041 inactivation of miR-34a and miR-34b/c by CpG methylation in colorectal,  
1042 pancreatic, mammary, ovarian, urothelial, and renal cell carcinomas and soft  
1043 tissue sarcomas." *Virchows Arch* **458**(3): 313-322. DOI: 10.1007/s00428-010-  
1044 1030-5  
1045  
1046 Wang, L., P. Bu, Y. Ai, T. Srinivasan, H. J. Chen, K. Xiang, S. M. Lipkin and X. Shen  
1047 (2016). "A long non-coding RNA targets microRNA miR-34a to regulate colon  
1048 cancer stem cell asymmetric division." *eLife* **5**. DOI: 10.7554/eLife.14620  
1049  
1050 Wang, L., H. J. Park, S. Dasari, S. Wang, J. P. Kocher and W. Li (2013). "CPAT:  
1051 Coding-Potential Assessment Tool using an alignment-free logistic regression  
1052 model." *Nucleic Acids Res* **41**(6): e74. DOI: 10.1093/nar/gkt006  
1053  
1054 Wang, X., J. Li, K. Dong, F. Lin, M. Long, Y. Ouyang, J. Wei, X. Chen, Y. Weng, T. He  
1055 and H. Zhang (2015). "Tumor suppressor miR-34a targets PD-L1 and functions  
1056 as a potential immunotherapeutic target in acute myeloid leukemia." *Cell Signal*  
1057 **27**(3): 443-452. DOI: 10.1016/j.cellsig.2014.12.003  
1058  
1059 Wickham, H. (2016). gtable: Arrange 'Grobs' in Tables. R package version 0.2.0.  
1060 <https://CRAN.R-project.org/package=gtable>  
1061  
1062 Wickham, H. (2017). scales: Scale Functions for Visualization. R package version  
1063 0.5.0. <https://CRAN.R-project.org/package=scales>  
1064  
1065 Wickham, H. (2017). tidyverse: Easily Install and Load the 'Tidyverse'. R package  
1066 version 1.2.1. <https://CRAN.R-project.org/package=tidyverse>  
1067  
1068 Wickham, L. H. a. H. (2017). rlang: Functions for Base Types and Core R and  
1069 'Tidyverse' Features. R package version 0.1.4. [https://CRAN.R-  
1070 project.org/package=rlang](https://CRAN.R-project.org/package=rlang)  
1071  
1072 Wickham, S. M. B. a. H. (2014). magrittr: A Forward-Pipe Operator for R. R  
1073 package version 1.5. <https://CRAN.R-project.org/package=magrittr>  
1074  
1075 Wilkins, D. gggenes: Draw Gene Arrow Maps in 'ggplot2'. R package version  
1076 0.2.0.9003. <https://github.com/wilkox/gggenes>  
1077  
1078 Xiao, N. (2017). liftr: Containerize R Markdown Documents. R package version  
1079 0.7. <https://CRAN.R-project.org/package=liftr>  
1080  
1081 Xie, Y. (2017). knitr: A General-Purpose Package for Dynamic Report Generation  
1082 in R. R package version 1.17. <https://yihui.name/knitr/>  
1083  
1084 Yang, P., Q. J. Li, Y. Feng, Y. Zhang, G. J. Markowitz, S. Ning, Y. Deng, J. Zhao, S.  
1085 Jiang, Y. Yuan, H. Y. Wang, S. Q. Cheng, D. Xie and X. F. Wang (2012). "TGF-beta-  
1086 miR-34a-CCL22 signaling-induced Treg cell recruitment promotes venous

1087 metastases of HBV-positive hepatocellular carcinoma." *Cancer Cell* **22**(3): 291-  
1088 303. DOI: 10.1016/j.ccr.2012.07.023  
1089  
1090 Yap, K. L., S. Li, A. M. Munoz-Cabello, S. Raguz, L. Zeng, S. Mujtaba, J. Gil, M. J.  
1091 Walsh and M. M. Zhou (2010). "Molecular interplay of the noncoding RNA ANRIL  
1092 and methylated histone H3 lysine 27 by polycomb CBX7 in transcriptional  
1093 silencing of INK4a." *Mol Cell* **38**(5): 662-674. DOI: 10.1016/j.molcel.2010.03.021  
1094  
1095 Yu, W., D. Gius, P. Onyango, K. Muldoon-Jacobs, J. Karp, A. P. Feinberg and H. Cui  
1096 (2008). "Epigenetic silencing of tumour suppressor gene p15 by its antisense  
1097 RNA." *Nature* **451**(7175): 202-206. DOI: 10.1038/nature06468  
1098  
1099 Zenz, T., J. Mohr, E. Eldering, A. P. Kater, A. Buhler, D. Kienle, D. Winkler, J. Durig,  
1100 M. H. van Oers, D. Mertens, H. Dohner and S. Stilgenbauer (2009). "miR-34a as  
1101 part of the resistance network in chronic lymphocytic leukemia." *Blood* **113**(16):  
1102 3801-3808. DOI: 10.1182/blood-2008-08-172254  
1103  
1104  
1105  
1106